

## FURTHER EVIDENCE FOR A SUPERMASSIVE BLACK HOLE MASS - PITCH ANGLE RELATION

JOEL C. BERRIER<sup>1,2,3,4</sup>, BENJAMIN L. DAVIS<sup>2</sup>, DANIEL KENNEFICK<sup>1,2</sup>, JULIA D. KENNEFICK<sup>1,2</sup>, MARC S. SEIGAR<sup>2,5</sup>, ROBERT SCOTT BARROWS<sup>2</sup>, MATTHEW HARTLEY<sup>1</sup>, DOUG SHIELDS<sup>1,2</sup>, MISTY C. BENTZ<sup>6</sup>, AND CLAUD H. S. LACY<sup>1,2</sup>

*Published in ApJ, 769, 132*

### ABSTRACT

We present new and stronger evidence for a previously reported relationship between galactic spiral arm pitch angle  $P$  (a measure of the tightness of spiral structure) and the mass  $M_{\text{BH}}$  of a disk galaxy's nuclear supermassive black hole (SMBH). We use an improved method to accurately measure the spiral arm pitch angle in disk galaxies to generate quantitative data on this morphological feature for 34 galaxies with directly measured black hole masses. We find a relation of  $\log(M/M_{\odot}) = (8.21 \pm 0.16) - (0.062 \pm 0.009)P$ . This method is compared with other means of estimating black hole mass to determine its effectiveness and usefulness relative to other existing relations. We argue that such a relationship is predicted by leading theories of spiral structure in disk galaxies, including the density wave theory. We propose this relationship as a tool for estimating SMBH masses in disk galaxies. This tool is potentially superior when compared to other methods for this class of galaxy and has the advantage of being unambiguously measurable from imaging data alone.

*Subject headings:* galaxies: fundamental parameters – galaxies: kinematics and dynamics – galaxies: nuclei – galaxies: spiral – galaxies: structure

### 1. INTRODUCTION

Since the existence of supermassive black holes (SMBHs) as a common, or even ubiquitous, component of galactic bulges was first recognized (Kormendy & Richstone 1995; Barth 2004; Kormendy 2004; Magorrian et al. 1998), increasingly successful attempts have been made to measure the mass of these objects. This has enabled astronomers to discover correlations between the mass of an SMBH and its host galaxy's mass or luminosity (Kormendy 1993; Kormendy & Richstone 1995; Magorrian et al. 1998; Marconi & Hunt 2003; Häring & Rix 2004). A number of features of the host galaxy have now been found to correlate to the mass of the black hole, giving rise to efforts to study the black holes by making measurements of features of the host galaxy even where the black hole is undetectable. Although many of these correlating features of the host galaxy require spectroscopy to measure, one which does not is the Sérsic index of the galaxy's bulge (Graham & Driver 2007). This correlation demonstrates the feasibility of estimating SMBH masses through imaging data alone. Here we verify and further refine a recently discovered relation between the spiral arm pitch angle of a galaxy and the mass of its SMBH, the  $M$ - $P$  relation (Seigar et al. 2008).

Our knowledge of SMBH masses in the universe has grown dramatically over the last decade, primarily due to high-resolution observations made with the *Hubble Space Telescope* (*HST*). These observations have shown that SMBHs reside not only in the cores of active galaxies, as has been be-

lieved for decades, but also in the centers of quiescent galaxies. Recent works have begun to explore the importance of the nuclear SMBHs in the evolution, or co-evolution, of its host galaxy (e.g. Magorrian et al. 1998; Ferrarese & Merritt 2000; Gebhardt et al. 2000; Marconi & Hunt 2003; Häring & Rix 2004; Springel et al. 2005; Hopkins et al. 2007; Rosario et al. 2010; Crenshaw et al. 2010; Treuthardt et al. 2012). As a result, any complete theory of galaxy formation has to produce SMBHs in the centers of massive galaxies (e.g. Silk & Rees 1998), and explain the evolution of SMBH mass over time.

Direct determination of SMBH mass depends on instrumentation which can observe the motion of stars, gas, and dust in the immediate vicinity of the black hole (Kormendy & Richstone 1995; Macchetto et al. 1997; Maciejewski & Binney 2001). This process is observationally expensive or impossible for distant galaxies. It is natural, therefore, that much time and effort have gone into the search for an indirect measure which can be used to give estimates of central SMBH mass. One remarkable indicator is the  $M_{\text{BH}}-\sigma$  relation, which relates the central SMBH mass ( $M_{\text{BH}}$ ) to the velocity dispersion in the central galactic bulge ( $\sigma$ ) (Ferrarese & Merritt 2000; Gebhardt et al. 2000). The  $M_{\text{BH}}-\sigma$  relation has led to considerable success estimating the SMBH mass for somewhat more distant galaxies, generally those whose cosmological redshift ( $z$ ) is  $z < 0.1$  (Heckman et al. 2004; Kauffmann et al. 2007). Thus the mass of the SMBH can be estimated for a wider range of galaxies. Nevertheless, as it is necessary to have spectroscopic measurements to estimate  $\sigma$  for the spheroidal component, it is still expensive in terms of telescope time. Additionally, measuring  $\sigma$  is more complex for disk galaxies than it is for ellipticals, since one must account for velocity dispersion associated with the motion of disk and bar stars intermingled with the velocity dispersion of the bulge stars, which is actually the correlating quantity (Hu 2008). Studies do suggest that the scatter in the  $M_{\text{BH}}-\sigma$  is significantly greater for disk galaxies than for ellipticals (Gültekin et al. 2009). Although projects such as the Sloan Digital Sky Survey have made progress in acquiring spectra of large numbers of galaxies, there have been few

<sup>1</sup> Department of Physics, University of Arkansas, 825 West Dickson Street, Fayetteville, AR 72701, USA

<sup>2</sup> Arkansas Center for Space and Planetary Sciences, University of Arkansas, 202 Old Field House, Fayetteville, AR 72701, USA

<sup>3</sup> Instituto de Astrofísica de Canarias, C/ Via Lactea s/n, E-38200 Tenerife, Spain

<sup>4</sup> Dept. Astrofísica, Universidad de La Laguna, E-38206 La Laguna, Tenerife, Spain

<sup>5</sup> Department of Physics and Astronomy, University of Arkansas at Little Rock, 2801 South University Avenue, Little Rock, AR 72204, USA

<sup>6</sup> Department of Physics and Astronomy, Georgia State University, Atlanta, GA 30303, USA

ways, up to now, to take advantage of the far larger catalogs of imaging data available from the public archives for the purpose of estimating black hole masses.

A far greater number of estimates can be made if features that are linked to the mass of SMBHs can be measured from imaging data. Several such relations have been explored, including those between black hole mass and bulge luminosity (e.g., Kormendy & Richstone 1995; Häring & Rix 2004), and Sérsic index and nuclear SMBH mass, (Graham & Driver 2007), among others. More recently, a relation between the central SMBH mass and the spiral arm pitch angle of its host galaxy has been discovered by examination of 27 disk galaxies with previously estimated SMBH masses (Seigar et al. 2008). The pitch angle of the spiral arms of the galaxy (essentially how tightly the spiral structure in the arms are wound) can be measured solely from images of the galaxy. There exist sets of images which cover significant field-of-view (FOV) to a considerable depth and look-back time for which this technique could provide estimates of the SMBH mass in a complete sample of spiral galaxies at much greater distances than have been possible hitherto, up to redshifts  $z \sim 1$  for especially deep images and favorable objects, but very likely to a redshift of  $z \sim 0.5$  for a significant sample of galaxies.

We may ask ourselves if such a relationship is expected from our understanding of galactic physics. The answer is in the affirmative. First, it has been shown empirically that there is a link between spiral arm pitch angle and the central mass concentration of galaxies (Seigar et al. 2005, 2006). It is generally agreed that a “strong correlation between central mass concentration and pitch angle [is] predicted by modal density wave theory,” (Grand et al. 2012) the dominant theory of spiral arm structure. Furthermore such a correlation between the size of the central bulge and the tightness of the spiral arm winding constitutes essentially the first significant, though at that point largely qualitative, observation of extragalactic astronomy, the basis of the Hubble classification. The notion that black hole mass depends on the mass of the central galactic bulge is now also widely established, as a result of observed correlations of black hole mass with both bulge velocity dispersion and bulge luminosity. Therefore black hole mass and spiral arm pitch angle should each measure the central mass concentration and should therefore correlate with each other quite strongly. Although the mechanism by which the correlation of black hole mass with central bulge mass is maintained is uncertain there are nevertheless highly plausible arguments why they should correlate (e.g., Silk & Rees 1998).

Shu (1984), who deals primarily with the case of density waves in the rings of Saturn naturally focuses on what can, in the context of galactic astronomy, be termed the bulge-dominated case. One has a central body (Saturn) whose mass far outweighs that of the material in the disk. The result is relatively straightforward to deal with theoretically, producing density waves in a tractable short wavelength approximation (density waves in Saturn’s rings typically have pitch angles measured in tenths of a degree). Even better the system is well understood observationally and there is excellent agreement between theory and observation. We may thus be very happy with the result given by Shu (1984) that the tangent of the pitch angle ( $i$ ) of the spiral pattern produced by density waves should be proportional to the ratio of the surface density of material in the disk to the total mass of the central body. Although Shu (1984) focuses mostly on the case of Saturn the formalism (the theory was, of course, developed in the

context of galactic spiral arms) is still approximately valid for the most bulge-dominated disk galaxies with relatively tightly wound spirals (small  $i$  and thus with the shortest wavelength density waves seen in galactic disks).

Naturally the case of galactic disks is much more complicated than that of Saturn’s rings, not least because of the self-gravity of the disk itself. Nor can we say that there is such close agreement between theory and observation in this case. Nevertheless there is quite good agreement and some success has been achieved in modeling individual galaxies with the density wave theory. An example is Roberts et al. (1975) which shows that the pitch angle in disk galaxies depends on the ratio of two radii, the half-mass radius, defined as the radius within which half the mass of the galaxy’s disk is contained, and the corotation radius, defined as the radius at which stars and other material bodies in the disk rotate at the same rate as the spiral pattern. Thus, once again, we see that the more concentrated the mass of the galaxy is toward the center (and thus the smaller is the half-mass radius), the tighter will be the spiral pattern.

It is not hard to show that the result of Roberts et al. (1975) is compatible with Shu (1984). If one reduces the former’s Toomre disk model to a very simple bulge (or planet) with a thin low-mass disk of uniform density and thickness, then the half-mass radius shrinks (and thus the pitch angle decreases) depending on the ratio of the central mass (the planet or bulge) to the surface mass density of the disk, which is the controlling factor in Shu (1984). Thus in bulge-dominated galaxies the pitch angle depends inversely on the mass of the central bulge. Disk-dominated galaxies, especially the extreme case of bulgeless galaxies, behave similarly in that their pitch angle correlates to the relative concentration of mass toward the center of the galaxy. Unfortunately, relatively little is known as yet about the relation between black hole mass and galaxy characteristics in disk-dominated galaxies, since relatively few black hole masses have been directly measured in such galaxies.

Indeed if there is no classical bulge, it is difficult to know how to interpret the  $M-\sigma$  or  $M$ -bulge luminosity relations at all. Clearly, further work will have to be done to understand the relation between disk dominated galaxies and their central black holes (if they have one). However, there are arguments which might suggest that there should still be a link between black hole mass and the mass of the central part of the disk. It is widely suspected that bulges are produced by mergers in which the central parts of galaxies become hotter and, heated past the point in which they maintain a flattened disk profile, adopt a bulge profile. If the central black hole mass does indeed correlate to the mass of this merger-created bulge, one might speculate that it would have previously (before the mergers) correlated to the mass of the central region of the disk, out of which material the post-merger bulge was presumably formed. But in that case the spiral arm pitch angle, pre-merger, would have also tended to correlate to the mass of the disk’s central region (which tends to control the value of the half-mass radius). Although it is not possible to say anything with certainty at this stage, it may prove that the mass-pitch angle relation could work for disk-dominated and bulgeless galaxies where other correlations ( $M-\sigma$ ,  $M-L$ ) would need to be reinterpreted. In the meantime, we can be fairly confident that for galaxies with classical bulges the pitch angle of the spiral arms should correlate well to the mass of that central bulge.

The dependence of pitch angle on central mass in the modal

density wave theory can be understood by analogy with standing waves on a string, since the modal density waves themselves constitute a standing-wave pattern. In the case of waves on a string, one expects the wavelength of the waves oscillating between the ends of the string to depend on the speed of propagation of the wave. This in turn depends on the ratio  $\rho/T$  where  $\rho$  is the density of the string and  $T$  is the tension in the string, the restoring force producing the wave phenomenon. In the modal theory, the density of material in the disk  $\sigma_o$  plays the role of the density of the string and the restoring force or tension is produced by the gravitational field of the massive central region of the galaxy. It is natural that the wavelength of the resultant spiral pattern should depend on the ratio of these two quantities.

It should be noted that the modal density wave theory is not the only theory which attempts to explain spiral arm structure in disk galaxies. Rivals include the swing amplification model of density wave theory (Kormendy 1981; Gerola & Seiden 1978; Seiden & Gerola 1979) and the Manifold theory (see below for selected references). It would be fair to say that the modal density wave theory is the most widely accepted but that each of these has significant support, at least for certain types of spiral galaxies. It has even been suggested that different galaxies (for instance, grand design versus flocculent) have different mechanisms explaining their spiral structure. Apart from a theory which proposes that spiral arms are the result of stochastic star formation operated upon by differential rotation all theories agree that there is a link between central mass and spiral arm pitch angle. The Toomre density wave theory differs from the modal theory primarily in denying that spiral arm structure lasts for longer than about a few rotational periods in a given galaxy (because in this theory there is no longstanding standing wave pattern). Pitch angle should vary with time in this theory, but should still obey a relation with the size of the central mass.

The Manifold theory of spiral structure is the most recently proposed of these theories (Kaufmann & Contopoulos 1996; Harsoula & Kalapotharakos 2009; Athanassoula et al. 2009b,a, 2010; Athanassoula 2012). This theory describes the spiral pattern as being the result of stars formed near the ends of a galaxy's bar moving into chaotic, highly eccentric orbits which nevertheless cause the stars to move along relatively narrow tubes known as manifolds. The global pattern produced by their motion along these manifolds gives rise to the observed spiral arms. The details of this theory are also subtle, but it is abundantly clear that the orbits, and therefore the manifolds, are controlled by the central mass concentration, as with all galactic orbits, and that therefore, once again, the pitch angle of the spiral arms should vary with the central mass of the galaxy (E. Athanassoula 2012, private communication).

Thus, we see that the primary theory for the formation of spiral structures, along with its two main competitors, are agreed that the mass of a central black hole should correlate with the mass of the central core of the galaxy. These theories demand that the mass of the central bulge should determine the pitch angle of the galaxy's spiral arms. Indeed, it is currently difficult to imagine a theory of spiral arm structure which does not demand a correlation with the central mass concentration, at least indirectly. But the two currently most actively pursued theories (modal density waves and manifold) both give the central mass a controlling influence on the mechanism which generates the pitch angle of the spiral pattern. It is not at all surprising, then, that we should find strong ev-

idence for such a concentration in actual observations, and with a notably low degree of scatter.

Finally, one needs look no further than the Hubble sequence to see an illustration of the connection between galactic morphologies and SMBH mass. The SMBH mass-bulge mass relation, when combined with the general pattern of larger bulges and tighter spiral arms as one moves from Sc to Sa in the Hubble sequence, demonstrates, at the very least, an indirect connection between these properties. Our view is that spiral arm pitch angle, which appears to be well correlated at least with SMBH mass, would be an excellent tool to probe the complex of correlated characteristics of spiral galaxies for several reasons. First, because it is measurable through imaging data alone. Second, it can take advantage of the great storehouse of publicly accessible archival data available. Finally, its measurement is independent of redshift, since logarithmic spirals remain self-similar no matter how they are scaled. In short, it may be possible that, for disk galaxies, we can gain information on the black hole masses for a significant number of spiral galaxies which previously could not have their masses estimated by other means.

Over the last few decades, it has become widely accepted that SMBHs and dark matter play influential, even dominant, roles in the evolution of galaxies. As neither black holes nor dark matter are directly observable in any part of the electromagnetic spectrum, information about them has been painstakingly obtained from observations of their gravitational effect on baryonic matter. Admittedly, Kormendy et al. (2011) suggested that SMBH mass does not correlate with galaxy disks, and Kormendy & Bender (2011) further suggest that a galaxy's dark matter halo does not have any direct correlation with the properties of the nuclear SMBH. However, Volonteri et al. (2011) and Booth & Schaye (2010, 2011) all provide counter results to those of Kormendy et al. (2011) and Kormendy & Bender (2011).

In this paper, we will re-examine the relationship of Seigar et al. (2008) and expand upon the sample used in that study by adding new measurements from other nearby spiral galaxies and active galactic nuclei (AGN). We will double the number of points used in the previous work, as well as update the method used in the measurement of the spiral arm pitch angles in Seigar et al. (2008) to that of Davis et al. (2012). We take advantage of SMBH mass data from a variety of measurement techniques including direct measurement of stellar and gas dynamics in the vicinity of the black hole, measurements based on available maser data for several objects and reverberation mapping. We also make use of a select set of data based on the  $M-\sigma$  relation, in an effort to deepen our understanding of the extent to which spiral arm structure correlates to central mass.

The structure of this paper is as follows: in Section 2, we outline the data we use in this work (including the observations and mass determinations) and the techniques used to measure morphological features of the observed galaxies. In Section 3, we assemble an updated SMBH mass-pitch angle relation using a variety of observational results and compare them across different subsamples. We also examine the use of Sérsic index as a means of estimating SMBH mass from galactic morphologies and compare that method with our results. In Section 4, we discuss the implications of this work and the usefulness of this method of SMBH mass estimation. Finally, in Section 5 we outline our final assessment of our results.

In this work, where necessary, we assume a cosmology of

$\Omega_\Lambda = 0.728$ ,  $\Omega_b = 0.0455$ ,  $\Omega_m h^2 = 0.1347$ , and  $H_0 = 70.4$  km s<sup>-1</sup> Mpc<sup>-1</sup>. This corresponds to the maximum likelihood cosmology from the combined *WMAP*+BAO+H0 results from the *WMAP* 7 data release (Komatsu et al. 2011).

## 2. METHODS

In this work, we investigate the relation between spiral arm pitch angle and central black hole mass using galaxies selected from a variety of sources with directly measured SMBH masses. Candidate galaxy images are selected from the available archival data. The sample listed in Table 1

includes spiral galaxies that have measurable spiral arm pitch angles and measured SMBH masses. For many of these galaxies, we also measure the Sérsic index to compare with the results of Graham & Driver (2007).

### 2.1. Sample Selection

The most desirable sample for us to use in this analysis is the one consisting of spiral galaxies with direct measurements of the SMBH mass through examination of either stellar or gas dynamics, or both, within the sphere of influence of the nuclear SMBH. We have available 10 galaxies with masses measured in this way. There are an additional 12 galaxies that have upper limits on their measured masses from stellar or gas dynamics and have no other estimations of their masses using other direct techniques as discussed below. We do not make use of these limits in constructing our relation, but we will later discuss the extent to which these limits are compatible with it. Nearly all (7 of 10) of these black hole mass measurements are for relatively large black holes, with masses  $M_{\text{BH}} > 1 \times 10^7 M_\odot$  in galaxies with relatively tightly wound spiral arms, with typically  $P < 15^\circ$ . If we notice that the mean value for pitch angle in nearby spiral galaxies is  $21.44^\circ$  (Davis et al. 2013), then all but one of these measurements, excluding limits, are for galaxies whose spiral arms have pitch angle less than this average. This means that we are missing the entire right-hand side of the distribution. That is to say, we have little information on the correlation for loosely wound spirals. It has been argued that spirals with the smallest black holes, i.e. the most loosely wound spirals, may not fit any correlation without considerable scatter (Kormendy et al. 2011), but substantial improvement in the relation would be possible with more data in the region from  $20^\circ$  to  $30^\circ$  in pitch angle. There is even more evidence that some of these galaxies may not contain black holes at all, but merely nuclear star clusters (or black holes within larger nuclear star clusters). This, however, is beyond the scope of our present discussion.

Fortunately, other techniques are available which provide a considerable number of further data points in order to expand our sample. These techniques provide several galaxies with smaller mass black holes than are available from the methods which can be employed in normal galaxies. We will incorporate data available from maser modeling and reverberation mapping.

The maser modeling data come from Lodato & Bertin (2003); Pastorini et al. (2007); Ishihara et al. (2001); Kondratko et al. (2006, 2008); Rodríguez-Rico et al. (2006); Greenhill et al. (2003b); Braatz & Gugliucci (2008); Greenhill et al. (2003a); Kuo et al. (2011). Observations of H<sub>2</sub>O masers in the vicinity of an active black hole are used to obtain circumnuclear disk rotation curves which can generate accurate measurements of the mass of SMBHs in these galaxies.

We also use 14 galaxies with mass estimates from reverberation mapping, 12 of which have not been measured using other direct methods. For discussions of this method see Peterson et al. (2005); Bentz et al. (2009a).

Taking these three categories together (direct measurements from stellar or gas dynamics, maser modeling and reverberation mapping) we have a final sample which includes 10 measurements using stellar or gas dynamics, 12 using maser modeling data, and 12 from reverberation mapping. Where the three samples overlap, we choose one of them as our preferred value (see Table 1 for details). This gives us a final sample of 34 spiral galaxies with direct measurements of their central black hole masses.

As a check on our work, we will consider a further data set of galaxies with more indirect measurements in our discussion. This includes 4 galaxies with lower limits set by the Edgington Limit, and 23 (3 also with direct measurements) with black hole masses estimated by the  $M$ - $\sigma$  relation of Ferrarese (2002). Although there are more recent publications on the  $M$ - $\sigma$  relation, we use this source for the purposes of drawing a comparison with our own previous work and postpone a more thorough discussion of the specific relation between  $\sigma$  and pitch angle to a future work. See Table 1 for full details on this extended data set. Also, please note that there is an overlap between some of the techniques mentioned above.

In certain cases we have multiple mass estimates or measurements of galaxies in our data set. Table 1 indicates which mass estimates we select for individual galaxies. Here we favor direct measurement techniques, such as stellar or gas dynamics, over techniques, such as maser modeling and reverberation mapping, which depend upon the black hole being active.

Whether maser modeling and reverberation mapping should be placed in a different category from other direct techniques is, of course, highly debatable. Clearly, they belong to a class of techniques which observe signals from material in direct orbit around the black hole itself, rather than with techniques such as the  $M$ - $\sigma$  relation, which merely correlate the mass of the black hole to some feature of the host galaxy. But for the purposes of this paper, it is useful to place maser modeling and reverberation mapping in a category together for two reasons. First, because both methods work exclusively for AGN and there has been a recent claim that the  $M$ - $\sigma$  relation, at least, is different for AGN than for normal galaxies (Park et al. 2012). Second, because these two methods cover a much greater stretch of the sample space than the other available direct methods, which tend to have had success exclusively for galaxies containing the most massive black holes.

A few exceptions to favoring direct stellar/gas based measurements exist. In cases where these are available we have chosen the most recent and reliable mass estimates available for the galaxy from among a variety of measurement techniques. Where these only produce an upper limit but not an estimated mass, we have chosen, where available, mass determinations from another method which provides a measurement of the mass with errors instead of just a limit. These differences are noted in Table 1. In Table 1, we include multiple entries for each object which has multiple different measurement types available in the literature. The measurements we prefer are labeled in the final column of the table.

Besides these general choices other exceptions are also made. NGC 5055 has a direct mass estimate in Gültekin et al. (2009) and Blais-Ouellette et al. (2004). Gültekin et al. (2009) suggests that the modeling used in the mass determi-

TABLE 1  
SAMPLE INFORMATION

Galaxy	$P$ (deg.)	Image Source	Filter	$\log(M_{\text{BH}}/M_{\odot})$	Measurement Type	Source	Preferred
3c120	$10.7 \pm 1.4$	Danish 1.54 (NED <sup>a</sup> )	$R$	$7.72^{+0.23}_{-0.23}$	Reverberation Mapping	1,2	Y
Ark 120	$5.4 \pm 0.6$	<i>HST</i> ACS (Bentz <sup>b</sup> )	F550M	$8.15^{+0.11}_{-0.11}$	Reverberation Mapping	1	Y
Circinus	$26.7 \pm 5.0$	<i>HST</i> WFPC2 (NED <sup>a</sup> )	F814W	$6.24^{+0.07}_{-0.08}$	Maser Modeling	3	Y
IC 342	$23.2 \pm 2.8$	VLA (NED <sup>a</sup> )	21 cm	$< 5.70$	Stars/Gas	4	
				$6.32^{+0.08}_{-0.09}$	$M-\sigma$	5	Y
IC 2560	$16.3 \pm 6.4$	2.5 m du Pont (CGS <sup>c</sup> )	$B$	$6.64^{+0.30}_{-0.30}$	Maser Modeling	6	Y
M 31	$8.5 \pm 1.3$	<i>GALEX</i> (NED <sup>a</sup> )	NUV	$8.15^{+0.22}_{-0.10}$	Stars/Gas	7	Y
				$7.59^{+0.08}_{-0.10}$	$M-\sigma$	5	
M 33	$34.5 \pm 8.6$	<i>Spitzer</i> IRAC (NED <sup>a</sup> )	IRAC 3.6 $\mu\text{m}$	$< 3.48$	Stars/Gas	8	
				$4.24^{+0.08}_{-0.09}$	$M-\sigma$	5	Y
Mrk 590	$8.5 \pm 3.3$	<i>HST</i> ACS (Bentz <sup>b</sup> )	F550M	$7.66^{+0.12}_{-0.12}$	Reverberation Mapping	1	Y
Mrk 79	$13.2 \pm 3.6$	Lick 1m (NED <sup>a</sup> )	$V$	$7.70^{+0.16}_{-0.16}$	Reverberation Mapping	1	Y
Mrk 817	$9.9 \pm 4.2$	<i>HST</i> ACS (Bentz <sup>b</sup> )	F550M	$7.69^{+0.08}_{-0.07}$	Reverberation Mapping	2	Y
Milky Way	$22.5 \pm 2.5$	Leiden/Argentine/Bonn (LAB) Survey (NED <sup>a</sup> )	21 cm	$6.63^{+0.04}_{-0.04}$	Stars/Gas	9	Y
				$6.84^{+0.04}_{-0.09}$	$M-\sigma$	5	
NGC 0253	$17.9 \pm 2.0$	2MASS 1.3m (NED <sup>a</sup> )	$K_s$	$7.01^{+0.30}_{-0.30}$	Maser Modeling	10	Y
NGC 0753	$13.2 \pm 0.6$	INT 2.5m (NED <sup>a</sup> )	$B$	$7.22^{+0.08}_{-0.09}$	$M-\sigma$	5	Y
NGC 1068	$20.6 \pm 4.5$	UKSchmidt (NED <sup>a</sup> )	468 nm	$6.95^{+0.02}_{-0.02}$	Maser Modeling	11	Y
NGC 1300	$10.3 \pm 1.8$	2.5 m du Pont (CGS <sup>c</sup> )	$B$	$7.85^{+0.29}_{-0.29}$	Stars/Gas	12	Y
NGC 1353	$13.7 \pm 2.3$	2MASS 1.3m (NED <sup>a</sup> )	$K_s$	$6.68^{+0.08}_{-0.09}$	$M-\sigma$	5	Y
NGC 1357	$11.8 \pm 4.8$	2.5 m du Pont (CGS <sup>c</sup> )	$B$	$7.22^{+0.08}_{-0.09}$	$M-\sigma$	5	Y
NGC 1417	$12.9 \pm 4.1$	2.5 m du Pont (CGS <sup>c</sup> )	$V$	$7.62^{+0.08}_{-0.10}$	$M-\sigma$	5	Y
NGC 2273	$17.5 \pm 7.2$	KPNO 2.1m (NED <sup>a</sup> )	$K$	$6.88^{+0.02}_{-0.02}$	Maser Modeling	13	Y
NGC 2639	$12.9 \pm 1.2$	<i>HST</i> (NED <sup>a</sup> )	F606W	$8.17^{+0.11}_{-0.15}$	$M-\sigma$	5	Y
NGC 2742	$32.5 \pm 7.9$	CAHA 2.2m (NED <sup>a</sup> )	1.25 $\mu\text{m}$	$5.92^{+0.08}_{-0.09}$	$M-\sigma$	5	Y
NGC 2841	$7.1 \pm 1.5$	<i>Spitzer</i> IRAC (NED <sup>a</sup> )	IRAC 3.6 $\mu\text{m}$	$8.00^{+0.09}_{-0.12}$	$M-\sigma$	5	Y
NGC 2903	$15.1 \pm 3.0$	Pal 60inch (NED <sup>a</sup> )	440 nm	$6.96^{+0.08}_{-0.09}$	$M-\sigma$	5	Y
NGC 2960	$7.5 \pm 1.7$	Palomar 48-inch Schmidt (NED <sup>a</sup> )	645 nm	$7.06^{+0.02}_{-0.02}$	Maser Modeling	13	Y
NGC 2998	$14.5 \pm 9.4$	KPNO 2.1m (NED <sup>a</sup> )	656.3 nm	$7.08^{+0.08}_{-0.09}$	$M-\sigma$	5	Y
NGC 3031	$15.4 \pm 8.6$	<i>Spitzer</i> IRAC (NED <sup>a</sup> )	IRAC 5.8 $\mu\text{m}$	$7.91^{+0.11}_{-0.07}$	Stars/Gas	14	Y
NGC 3145	$7.2 \pm 1.3$	2.5 m du Pont (CGS <sup>c</sup> )	$B$	$7.85^{+0.09}_{-0.11}$	$M-\sigma$	5	Y
NGC 3198	$30.0 \pm 6.7$	KPNO 2.1m CFIM (NED <sup>a</sup> )	700 nm	$6.10^{+0.08}_{-0.09}$	$M-\sigma$	5	Y
NGC 3223	$10.9 \pm 2.2$	2.5 m du Pont (CGS <sup>c</sup> )	$B$	$7.81^{+0.09}_{-0.11}$	$M-\sigma$	5	Y
NGC 3227	$12.9 \pm 9.0$	JKT (NED <sup>a</sup> )	H $\alpha$	$7.33^{+0.18}_{-0.10}$	Stars/Gas	15	Y
				$7.60^{+0.24}_{-0.24}$	Reverberation Mapping	16	
NGC 3310	$22.7 \pm 9.1$	<i>HST</i> WFPC2 (NED <sup>a</sup> )	F814W	$< 7.62$	Stars/Gas	17	Y
NGC 3351	$11.1 \pm 1.8$	CTIO 4.0m (NED <sup>a</sup> )	$B$	$< 6.96$	Stars/Gas	18	Y
NGC 3367	$36.8 \pm 5.3$	OAN Martir 2.12m (NED <sup>a</sup> )	$I$	$> 5.20$	Eddington	19	Y
NGC 3368	$14.0 \pm 1.4$	VATT Lennon 1.8m (NED <sup>a</sup> )	$R$	$6.90^{+0.08}_{-0.10}$	Stars/Gas	17,20	Y

nation is very uncertain. In this case we have chosen to fall back on the mass of the black hole derived from the  $M-\sigma$  relation in Ferrarese (2002). In the case of NGC 4395, we have decided to use the more recent reverberation mapping data and corresponding mass estimate over the mass estimate based on combining upper and lower limits set on the mass in Filippenko & Ho (2003).

## 2.2. Imaging Data

The majority of images used for measuring pitch angles came from the NASA/IPAC Extragalactic Database (NED)<sup>7</sup>. This resulted in the implementation of a wide range of wavelength images; anywhere from far-ultraviolet (FUV) to 21 cm H emission. See Table 1 for details on each individual galaxy. Despite this broad range of wavelength imaging, recent results show that galactic pitch angle measurements are independent of the wavelength of the image (Seigar et al. 2006; Davis et al. 2012), or at least not strongly dependent (Grosbol & Patsis 1998), especially in the UV to near-IR (NIR) wavelength regimes. Although this correlation has not been tested in the

mid-IR to radio regimes, we can assume that it still applies for several reasons. For the mid-IR regime, i.e., where we have used *Spitzer*/IRAC 5.8  $\mu\text{m}$  and 8.0  $\mu\text{m}$  imaging, star formation is being traced, and so this should give a similar pitch angle to a  $B$ -band image. In two cases we resort to 21 cm data to measure pitch angles. While there is currently no empirical evidence correlating 21 cm pitch angles to optical or NIR pitch angles, there is no reason to suggest that the 21 cm data are not influenced in a similar way by the underlying density wave.

When given the option, the imaging with the best resolution was used (typically  $B$ -band images). According to Thornley (1996), a spiral that appears flocculant in the  $B$  band may appear to have a weak grand design spiral in the NIR. In these cases, NIR imaging was investigated (typically from 2MASS, Jarrett et al. 2000, or *Spitzer* images).

Some galaxies in our sample had pitch angles measured in Davis et al. (2012), where the method of measuring pitch angle we use here is described. Some of these previously measured pitch angles, reported in Davis et al. (2012), used high-quality imaging from the Carnegie-Irvine Galaxy Sur-

<sup>7</sup> <http://ned.ipac.caltech.edu/>

TABLE 1  
(CONTINUED)

Galaxy	$P$ (deg.)	Image Source	Filter	$\log(M_{\text{BH}}/M_{\odot})$	Measurement Type	Source	Preferred
NGC 3393	$13.1 \pm 2.5$	CTIO 0.9m (NED <sup>a</sup> )	$B$	$7.52^{+0.03}_{-0.03}$	Maser Modeling	21,22	Y
NGC 3516	$10.6 \pm 4.3$	<i>HST</i> WFPC2 (NED <sup>a</sup> )	500.7 nm	$7.61^{+0.18}_{-0.18}$	Reverberation Mapping	1	Y
NGC 3621	$12.7 \pm 1.2$	2.5 m du Pont (CGS <sup>c</sup> )	$B$	$> 3.60$	Eddington	23	Y
NGC 3783	$10.5 \pm 4.8$	LCO 2.5m (NED <sup>a</sup> )	$K$	$7.45^{+0.13}_{-0.13}$	Reverberation Mapping	1	Y
NGC 3938	$22.4 \pm 7.2$	KPNO 2.1m CFIM (NED <sup>a</sup> )	$B$	$> 4.26$	Eddington	19	Y
NGC 3982	$14.0 \pm 0.4$	MaunaKea2.24m (NED <sup>a</sup> )	$R$	$< 7.93$	Stars/Gas	18	Y
NGC 3992	$6.2 \pm 6.1$	MaunaKea2.24m (NED <sup>a</sup> )	$B$	$< 7.78$	Stars/Gas	18	Y
NGC 4041	$23.3 \pm 8.2$	Palomar 48-inch Schmidt (NED <sup>a</sup> )	645 nm	$< 7.33$	Stars/Gas	24	Y
NGC 4051	$29.1 \pm 4.9$	MaunaKea2.24m (NED <sup>a</sup> )	$B$	$6.24^{+0.12}_{-0.16}$	Reverberation Mapping	32	Y
NGC 4062	$12.4 \pm 1.4$	1.8m Perkins (NED <sup>a</sup> )	$B$	$6.63^{+0.08}_{-0.09}$	$M-\sigma$	5	Y
NGC 4151	$11.8 \pm 1.8$	VLA (NED <sup>a</sup> )	21 cm	$7.66^{+0.09}_{-0.05}$	Stars/Gas	25	Y
			21 cm	$7.64^{+0.11}_{-0.11}$	Reverberation Mapping	16	
NGC 4258	$7.7 \pm 4.2$	<i>Spitzer</i> IRAC (NED <sup>a</sup> )	IRAC 8.0 $\mu\text{m}$	$7.90^{+0.25}_{-0.25}$	Stars/Gas	17	Y
				$7.59^{+0.01}_{-0.01}$	Maser Modeling	26,27	
				$7.48^{+0.08}_{-0.10}$	$M-\sigma$	5	
NGC 4303	$13.5 \pm 4.6$	1.3m McGraw-Hill (NED <sup>a</sup> )	$B$	$6.92^{+0.29}_{-1.14}$	Stars/Gas	17	Y
NGC 4321	$21.8 \pm 3.6$	KP 2.1m CFIM (NED <sup>a</sup> )	$R$	$< 7.46$	Stars/Gas	18	
			$R$	$6.47^{+0.08}_{-0.09}$	$M-\sigma$	5	Y
NGC 4388	$26.2 \pm 8.2$	KPNO 2.3m (NED <sup>a</sup> )	$K_s$	$6.93^{+0.01}_{-0.01}$	Maser Modeling	13	Y
NGC 4395	$35.2 \pm 6.8$	<i>GALEX</i> (NED <sup>a</sup> )	FUV	$5.56^{+0.12}_{-0.16}$	Reverberation Mapping	28	Y
NGC 4450	$9.1 \pm 3.1$	KP 2.1m CFIM (NED <sup>a</sup> )	$B$	$< 8.07$	Stars/Gas	18	Y
NGC 4501	$12.7 \pm 1.4$	KP9 t2ka (NED <sup>a</sup> )	$R$	$< 7.98$	Stars/Gas	18	Y
NGC 4536	$14.8 \pm 7.9$	KP 2.1m CFIM (NED <sup>a</sup> )	$R$	$> 3.68$	Eddington	19	Y
NGC 4548	$25.6 \pm 6.6$	JKT (NED <sup>a</sup> )	$B$	$< 7.55$	Stars/Gas	18	Y
NGC 4593	$20.2 \pm 2.7$	2.5 m du Pont (CGS <sup>c</sup> )	$I$	$6.97^{+0.14}_{-0.14}$	Reverberation Mapping	33	Y
NGC 4800	$21.5 \pm 3.2$	KP9 t2ka (NED <sup>a</sup> )	$R$	$< 7.53$	Stars/Gas	18	Y
NGC 5033	$16.5 \pm 5.6$	KP 2.1 CFIM (NED <sup>a</sup> )	$B$	$7.24^{+0.08}_{-0.09}$	$M-\sigma$	5	Y
NGC 5055	$14.9 \pm 6.9$	<i>Spitzer</i> IRAC (NED <sup>a</sup> )	IRAC 5.8 $\mu\text{m}$	$6.90^{+0.08}_{-0.08}$	$M-\sigma$	5	Y
NGC 5495	$27.8 \pm 1.2$	UK 48-inch Schmidt (NED <sup>a</sup> )	468 nm	$7.03^{+0.18}_{-0.30}$	Maser Modeling	21	Y
NGC 5548	$15.0 \pm 2.5$	<i>HST</i> (NED <sup>a</sup> )	F606W	$7.80^{+0.10}_{-0.10}$	Reverberation Mapping	34,35	Y
NGC 6323	$11.8 \pm 3.4$	Palomar 48-inch Schmidt (NED <sup>a</sup> )	645 nm	$6.97^{+0.00}_{-0.00}$	Maser Modeling	13	Y
NGC 6926	$17.5 \pm 5.5$	2MASS (NED <sup>a</sup> )	$K_s$	$6.77^{+0.26}_{-0.74}$	Maser Modeling	29	Y
NGC 7331	$22.2 \pm 4.2$	<i>Spitzer</i> IRAC (NED <sup>a</sup> )	IRAC 3.6 $\mu\text{m}$	$7.50^{+0.08}_{-0.10}$	$M-\sigma$	5	Y
NGC 7469	$28.5 \pm 4.3$	<i>HST</i> NIC2 (NED <sup>a</sup> )	F110W	$< 7.73$	Stars/Gas	16	
				$7.06^{+0.11}_{-0.11}$	Reverberation Mapping	1	Y
NGC 7582	$14.7 \pm 7.4$	ESO 1m Schmidt (NED <sup>a</sup> )	$R$	$7.74^{+0.17}_{-0.18}$	Stars/Gas	30	Y
NGC 7606	$11.3 \pm 1.2$	2.5 m du Pont (CGS <sup>c</sup> )	$V$	$7.27^{+0.08}_{-0.09}$	$M-\sigma$	5	Y
UGC 3789	$10.5 \pm 4.8$	Palomar 48-inch Schmidt (NED <sup>a</sup> )	645 nm	$6.96^{+0.30}_{-0.26}$	Maser Modeling	31	Y

NOTE. — Column 1: galaxy name. Column 2: pitch angle (degrees); the pitch angle for the Milky Way comes from Levine et al. (2006). Column 3: image source *a* Images taken from NASA Extragalactic Database (NED). *b* Images provided by Misty Bentz. *c* The pitch angles for Carnegie-Irvine Galaxy Survey (CGS) galaxies come from Davis et al. (2012). Column 4: image filter. Column 5  $\log(M_{\text{BH}}/M_{\odot})$ . Column 6: measurement type. Column 7: mass measurement source. Column 8: preferred measurement. **References:** (1) Peterson et al. 2004; (2) Bentz et al. 2009b; (3) Greenhill et al. 2003a; (4) Böker et al. 1999; (5) Ferrarese 2002; (6) Ishihara et al. 2001; (7) Bender et al. 2005; (8) Merritt et al. 2001; (9) Gillessen et al. 2009; (10) Rodríguez-Rico et al. 2006; (11) Lodato & Bertin 2003; (12) Atkinson et al. 2005; (13) Kuo et al. 2011; (14) Devereux et al. 2003; (15) Davies et al. 2006; (16) Hicks & Malkan 2008; (17) Pastorini et al. 2007; (18) Sarzi et al. 2002; (19) Satyapal et al. 2008; (20) Nowak et al. 2010b; (21) Kondratko et al. 2006; (22) Kondratko et al. 2008; (23) Satyapal et al. 2007; (24) Marconi et al. 2003; (25) Onken et al. 2007; (26) Herrnstein et al. 2005; (27) Miyoshi et al. 1995; (28) Peterson et al. 2005; (29) Greenhill et al. 2003b; (30) Wold et al. 2006; (31) Braatz & Gugliucci 2008; (32) Denney et al. 2010; (33) Denney et al. 2006; (34) Bentz et al. 2007; (35) Bentz et al. 2009c.

vey (CGS;<sup>8</sup> Ho et al. 2011), providing a desirable set of input imaging for our two-dimensional Fast Fourier transform software, named 2DFFT. Images highlighting the sharpest detail in spiral arm structure were primarily selected (typically  $B$ -band images). See Davis et al. (2012) for details on these images.

Finally, for some galaxies with AGN in our sample, we have consulted high-resolution *HST* ACS F550M images of reverberation-mapped AGN host galaxies, used in Bentz et al. (2009a). Many of these images did not reveal any spiral structure because of the bright nucleus or the small FOV. In these cases we resorted to ground-based, wider FOV images to measure pitch angles. In the end, three galaxies had pitch

angles measured using *HST* data from Bentz et al. (2009a).

### 2.3. Measuring Pitch Angles

We use the method described in Davis et al. (2012) to accurately measure the pitch angles of the 34 galaxies with direct mass measurements that comprise our sample, plus additional 33 galaxies with mass limits or  $M-\sigma$  estimates used in our extended data set. This technique is an extension of the method described in Saraiva Schroeder et al. (1994), which utilizes a 2DFFT algorithm to measure the pitch angle between a user defined inner and outer radius on a deprojected image of a spiral galaxy. For more details, see Puerari & Dottori (1992); Puerari et al. (2000). Galaxies are deprojected by assuming that the disk galaxy, when face-on, will have circular isophotes. Although Ryden (2004) has shown that disk galax-

<sup>8</sup> <http://cgs.obs.carnegiescience.edu/>

ies do have an intrinsic ellipticity, it is relatively small, and Davis et al. (2012) have shown that small errors in the measured axial ratio of galaxies do not affect the measured spiral arm pitch angle.

The extension to this method in Davis et al. (2012) eliminates the user defined inner radius in favor of measuring the pitch angle over all possible inner radii, thus allowing the user to examine the results of the Fourier analysis for long regions over which changing the inner radius of the transformed region of the data does not affect the measured pitch angle. This provides a far more accurate measurement of the pitch angle of the galaxy than single measurement techniques utilizing individual inner radii, as well as providing us a means of examining the consistency of the logarithmic structure of the spiral arms. For further details on this technique, see Davis et al. (2012).

There are many advantages for using this method. First, it helps us eliminate a great deal of uncertainty involved in measuring the pitch angles of galaxies. Instead of simply assuming that the galaxy's spiral is logarithmic, it provides some check on the extent to which that is true by varying the region over which the Fourier analysis is performed. If a departure from logarithmic behavior is found (most commonly in a change of the spiral arm structure in the very outer regions of the galaxy) then the user can select a region over which the behavior is consistent and use the pitch angle associated with that region. In our case this means we are able to focus on the inner region where we expect that the behavior of the spiral arm structure will be more strongly affected by the mass of the central concentration. Additionally, both Seigar et al. (2006) and Davis et al. (2012) established the consistency between *B*-band and NIR-band pitch angles, demonstrating that pitch angle does not depend measurably on the band chosen for imaging. The results of Davis et al. (2012) demonstrate that the pitch angles of the galaxies in that sample appear to be generally independent of the band of the observations, at least within the uncertainties of the reported pitch angles. Only one group have so far reported such an effect (Grosbol & Patsis 1998) and they agree that the amount of the variation (which is visible in only three of their studied galaxies) is no more than seven degrees between *K*-band and *B*-band images. Thus, with this method one may measure the spiral arm pitch angle for nearly all late-type galaxies, limited by little more than the requirement, which should be random and unbiased, that the galaxy is not close to edge-on to our line of sight.

One obvious variation in the appearance of spiral arm galaxies is the distinction between flocculant and grand design spirals. Flocculant spirals lack the regularity in arm segments seen in other spirals. Because of this lack of long stretches of continuous arms, measuring a pitch angle for them is not so straightforward, at least using manual methods, as it is in the case of grand design spirals. However, our method permits the user to establish whether there is, nevertheless, a consistent spiral pattern, with measurable pitch angle and number of arms, over the whole disk. Only in a handful of cases in this sample does a flocculant galaxy present particular difficulties to our method, as evidenced by a larger than usual error quoted.

It has been argued (for instance by Seiden & Gerola 1982) that flocculant spiral arms may be produced by a different physical process than grand design spiral arms (regions of self-propagating star-formation acted upon by differential rotation in the former case, spiral density waves in the latter).

It is also noteworthy that galaxies which are flocculant in the *B* band may show a grand design pattern in the *R* band (Thornley 1996) due to the potentially different origins of the spiral structure in flocculant galaxies and the old stellar population in the redder bands tracing the spiral density waves (Seigar & James 1998). It appears that though there may be a large difference in detailed appearance (thus in one band, the image seems flocculant, but not in another) there are only small differences in measurable structure, the spiral arm pitch angle. This is certainly suggestive of a similar underlying cause for the different varieties of spiral structure. In our case, where we did find large errors in the measurement of flocculant spirals we have preferred to use NIR images for such galaxies, which seems to reduce measurement errors noticeably.

#### 2.4. Sérsic Index

Sérsic index (Sérsic 1963) has been proposed as another observable feature which correlates with SMBH mass (Graham & Driver 2007). Like pitch angle, it can be measured using only imaging data. It may be that a combination of these two approaches, pitch angles for spiral galaxies and Sérsic index for ellipticals, lenticulars, and edge-on spirals will enable observers to estimate the SMBH mass function in normal galaxies out to considerable distances. Although Sérsic indices can be measured for face-on spirals, doing so involves a complex process of disentangling bulge from disk and bar components of the galaxy. It is likely that measuring the pitch angle of such galaxies will be easier and more accurate. However, any such campaign will certainly demand some analysis of how well the two approaches agree in their estimate of central black hole mass. In order to make a comparison between our pitch-angle-derived masses and the work of Graham & Driver (2007), we must calculate the Sérsic index for the galaxies in our sample. We have done so for 31 galaxies, and further 4 have been taken from the literature (Graham & Driver 2007; Kent et al. 1991; Nowak et al. 2010a). We have excluded AGN from the sample of galaxies with measured Sérsic index due to the difficulties presented by the bright nucleus.

The Sérsic profile relates how the brightness of a galaxy falls off with distance from the center. It is of the form:

$$I(R) = I_e \exp^{-b_n[(R/R_e)^n - 1]}, \quad (1)$$

where  $R$  is the radius of the isophote,  $R_e$  is the radius which encloses half of the light of the galaxy,  $I_e$  is the intensity at this radius,  $b_n$  is fitted with the function

$$b_n = 1.9992n - 0.3271 \quad (2)$$

(Graham & Driver 2005), and lastly,  $n$  is the Sérsic index. The Sérsic index is also a measure of the concentration of the galaxy, defined as the amount of light enclosed by some fraction (usually taken to be around a third) of the effective radius divided by the amount of light enclosed by the effective radius, which by definition is half the light of the bulge.

We measure the Sérsic index by fitting the surface brightness contours produced by Image Reduction and Analysis Facility routine *Ellipse* (Tody 1986; Jedrzejewski 1987). A bulge/disk decomposition is performed on these data and a Sérsic profile (plus exponential disk for spirals) is fit to the resultant data.

It was shown in Graham et al. (2001) that light concentration correlates strongly with black hole mass. Later,

TABLE 2  
SAMPLE MORPHOLOGY AND SÉRSIC INDEX

Galaxy	Morphology	Sérsic Index	$\log(M_{\text{BH}}/M_{\odot})$	Source
IC 2560	(R')SB(r)b	$1.19^{+0.24}_{-0.20}$	$6.994^{+0.045}_{-0.077}$	1
M31	SA(s)b	$3.19^{+0.64}_{-0.53}$	$8.081^{+0.327}_{-0.351}$	1
Milky Way	S?	$1.32^{+0.22}_{-0.26}$	$7.055^{+0.081}_{-0.067}$	2
NGC 0253	SAB(s)c	$1.17^{+0.23}_{-0.19}$	$6.985^{+0.039}_{-0.073}$	1
NGC 0753	SAB(rs)bc	$1.58^{+0.32}_{-0.26}$	$7.190^{+0.093}_{-0.113}$	1
NGC 1357	SA(s)ab	$1.48^{+0.30}_{-0.25}$	$7.137^{+0.083}_{-0.107}$	1
NGC 1417	SAB(rs)b	$1.56^{+0.31}_{-0.26}$	$7.179^{+0.092}_{-0.113}$	1
NGC 2903	SAB(rs)bc	$3.28^{+0.66}_{-0.56}$	$8.128^{+0.347}_{-0.340}$	1
NGC 2998	SAB(rs)c	$2.27^{+0.45}_{-0.38}$	$7.577^{+0.199}_{-0.203}$	1
NGC 3031	SA(s)ab	$3.23^{+0.54}_{-0.65}$	$8.102^{+0.401}_{-0.279}$	3
NGC 3145	SB(rs)bc	$1.58^{+0.32}_{-0.26}$	$7.190^{+0.093}_{-0.119}$	1
NGC 3198	SB(rs)c	$1.33^{+0.27}_{-0.22}$	$7.060^{+0.060}_{-0.091}$	1
NGC 3227	SAB(s)a pec	$2.52^{+0.50}_{-0.38}$	$7.718^{+0.235}_{-0.174}$	1
NGC 3310	SAB(r)bc pec	$1.89^{+0.32}_{-0.32}$	$7.362^{+0.156}_{-0.156}$	1
NGC 3351	SB(r)b	$2.40^{+0.48}_{-0.40}$	$7.651^{+0.217}_{-0.223}$	1
NGC 3367	SB(rs)c	$0.98^{+0.20}_{-0.16}$	$6.914^{+0.023}_{-0.065}$	1
NGC 3368	SAB(rs)ab	$2.35^{+0.00}_{-0.00}$	$7.622^{+0.030}_{-0.030}$	4
NGC 3621	SA(s)d	$1.89^{+0.38}_{-0.35}$	$7.362^{+0.144}_{-0.156}$	1
NGC 3938	SA(s)c	$1.45^{+0.24}_{-0.24}$	$7.121^{+0.102}_{-0.102}$	1
NGC 3982	SAB(r)b:	$2.14^{+0.43}_{-0.36}$	$7.504^{+0.180}_{-0.189}$	1
NGC 3992	SB(rs)bc	$1.40^{+0.28}_{-0.15}$	$7.095^{+0.068}_{-0.075}$	1
NGC 4041	SA(rs)bc	$0.74^{+0.13}_{-0.12}$	$6.876^{+0.015}_{-0.066}$	1
NGC 4051	SAB(rs)bc	$2.18^{+0.44}_{-0.36}$	$7.527^{+0.182}_{-0.196}$	1
NGC 4258	SAB(s)bc	$2.04^{+0.34}_{-0.41}$	$7.447^{+0.206}_{-0.138}$	3
NGC 4303	SAB(rs)bc	$0.79^{+0.16}_{-0.13}$	$6.877^{+0.013}_{-0.064}$	1
NGC 4321	SAB(s)bc	$1.86^{+0.37}_{-0.31}$	$7.345^{+0.136}_{-0.150}$	1
NGC 4450	SA(s)ab	$1.34^{+0.27}_{-0.22}$	$7.065^{+0.061}_{-0.091}$	1
NGC 4501	SA(rs)b	$2.28^{+0.46}_{-0.38}$	$7.583^{+0.199}_{-0.209}$	1
NGC 4536	SAB(rs)bc	$2.27^{+0.17}_{-0.14}$	$7.577^{+0.052}_{-0.054}$	1
NGC 4548	SB(rs)b	$1.58^{+0.32}_{-0.26}$	$7.190^{+0.084}_{-0.119}$	1
NGC 4593	(R)SB(rs)b	$2.40^{+0.48}_{-0.40}$	$7.651^{+0.217}_{-0.223}$	1
NGC 5033	SA(s)c	$1.93^{+0.39}_{-0.32}$	$7.385^{+0.146}_{-0.133}$	1
NGC 5495	(R')SAB(r)c	$0.69^{+0.14}_{-0.12}$	$6.881^{+0.016}_{-0.071}$	1
NGC 6926	SB(s)bc pec	$1.77^{+0.35}_{-0.30}$	$7.295^{+0.126}_{-0.138}$	1
UGC 3789	(R)SA(r)ab	$0.95^{+0.19}_{-0.15}$	$6.905^{+0.019}_{-0.063}$	1

NOTE. — Column 1: galaxy name. Column 2: galaxy morphology taken from NED. Column 3: Sérsic index. Column 4:  $\log(M_{\text{BH}}/M_{\odot})$  derived from each galaxy's measured Sérsic index using the relation of Graham & Driver (2007). Column 5: source of Sérsic index measurement. **References:** (1) This work; (2) Kent et al. 1991; (3) Graham & Driver 2007; (4) Nowak et al. 2010a.

Graham & Driver (2007) found a log relation between Sérsic index and black hole mass. This correlation is of the form

$$\log(M_{\text{bh}}) = (7.98 \pm 0.09) + (3.70 \pm 0.46) \log(n/3) - (3.10 \pm 0.84) [\log(n/3)]^2. \quad (3)$$

Thus the Sérsic index provides an estimate of SMBH masses through images of galactic bulges. We will make comparisons between our technique and the results of Graham & Driver (2007) in Section 3.7. The Sérsic indices for several galaxies in our sample, along with corresponding mass estimates from the relation of Graham & Driver (2007) are included in Table 2.

### 3. RESULTS

#### 3.1. An Updated SMBH Mass–Pitch Angle Relation

As discussed above, we chose our sample to include spiral galaxies whose central black hole masses have been measured using a direct technique. We define a direct technique to be one which measures the motions and positions of material in orbit around the black hole or directly within its sphere of

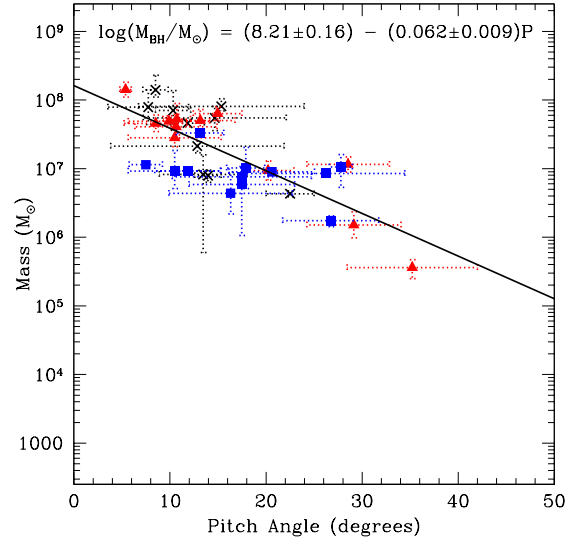


FIG. 1.— Black hole mass vs. pitch angle for all spiral galaxies with directly measured black hole masses available. The best linear fit to this data is illustrated and gives the following relation  $\log(M_{\text{BH}}/M_{\odot}) = (8.21 \pm 0.16) - (0.062 \pm 0.009)P$ . The fit has a reduced  $\chi^2 = 4.68$  with a scatter of 0.38 dex. Black hole masses measured using stellar and gas dynamics techniques are labeled with black  $\times$ 's (10 points), reverberation mapping masses with red triangles (12 points), and maser measurements with blue squares (12 points).

influence. This definition encompasses quite a few different methods. Not all are equally accurate or reliable, but for our purposes they all have the important distinction that they do extract information from signals emitted by material in the direct gravitational influence of the black hole.

Combining these three samples, stellar and gas dynamics, maser modeling, and reverberation mapping, we have a total sample of 34 objects. Fitting these data points (Figure 1), we find an updated SMBH  $M$ – $P$  relation of

$$\log(M_{\text{BH}}/M_{\odot}) = (8.21 \pm 0.16) - (0.062 \pm 0.009)P, \quad (4)$$

where  $P$  is the absolute value of the measured pitch angle of the galaxy in degrees. Please note that the sign of a pitch angle measurement merely represents the chirality of the galaxy based upon the user's line of sight and is unimportant. This fit has a  $\chi^2 = 4.68$  and a scatter of 0.38 dex. This result is consistent with the previous result of Seigar et al. (2008). It is encouraging that, with significantly more data available, the scatter has remained unchanged. This value is less than the scatter of spiral galaxies about the  $M$ – $\sigma$  relation of  $\sim 0.56$  dex from Gültekin et al. (2009). A Pearson rank correlation coefficient test produces a coefficient of  $-0.81$ , a strong anti-correlation. This result has a significance of 99.7%, a  $3\sigma$  result.

As discussed above, the scatter in this relation is comparable to other relationships. A possible reason for the reduced scatter in this relationship, when compared with Gültekin et al. (2009), is that the measurement of  $\sigma$  in spiral galaxies requires that one distinguishes the contributions of the galactic bulge from other stellar components such as the disk or bar. Where the galaxy has an active nucleus, the region over which  $\sigma$  is measured is usually obscured and a proxy (some spectral line or lines in the AGN spectrum) must be used. Many of the galaxies in this sample have AGNs in their nuclei.

In the case of bulge luminosity, the presence of an AGN can sometimes be overcome, but when the galaxy is a disk galaxy one must undertake decomposition of the light from



the galaxy, fitting multiple components to the luminosity profile (bulge, disk, and bar are the main components). Once again, the presence of unresolved nuclear flux (e.g., AGN or LINER or even nuclear star cluster) will create difficulties in determining bulge luminosity or Sérsic index. Some algorithms have been used to measure large numbers of galactic bulge luminosities for the purposes of bulge mass estimates or measurements of Sérsic index (e.g. de Souza et al. 2004). Automated codes may have difficulties disentangling the unresolved nucleus and the bulge, especially with ground-based seeing of  $\sim 1''$  for any galaxies that are not nearby. The method of Davis et al. (2012) is unaffected by this issue. In the case of measurements of spiral arm pitch angle, we examine a component which is unambiguous in spiral galaxies in much the same way that  $\sigma$  is unambiguous in elliptical galaxies. The method of Davis et al. (2012) requires minimal image processing to yield a measurement of the pitch angle, requiring only a deprojection and cropping of the image and the locations of the central pixel and galactic edge.

For the purposes of estimating black hole masses on the basis of pitch angle measurements of galactic spiral arms, we propose to use this fit based on direct measurements of SMBH mass.

### 3.2. Comparison with the Previous $M$ - $P$ Relation

In our previous work (Seigar et al. 2008), black hole masses derived from measurements of  $\sigma$ , the velocity dispersion in the core bulge region, all reported in Ferrarese (2002), were used. This was largely because of the relative scarcity of direct measurements of black hole masses in spiral galaxies. Since then the available number of direct measurements has increased by over a factor of two. We therefore exclude any  $\sigma$ -derived masses from the correlation fit developed here, as it is not a direct measurement of black hole mass. Indeed, the correlation between  $\sigma$  and black hole mass which we use is based upon a fit using some of the objects we include in our sample. Later in this section we will include those same  $\sigma$ -derived values in a fit which we derive primarily to check how closely our results agree with the results reported in that earlier paper (Seigar et al. 2008). Additionally, when we compare our results with these indirect values it provides a useful check on the overall validity of our correlation. This is especially true because the number of black hole masses measured by direct techniques which are near or below a million solar masses is very small. Including some  $\sigma$  values does provide a useful check on the slope of the fit by providing some extra evidence at the low mass end of the graph. In any case the value of our fit, including the  $\sigma$ -derived values, agrees very closely with the one reported in the earlier paper.

It is important to note that while the updated fit reported here differs from the one in Seigar et al. (2008), though only to a minor degree, the discrepancy is not caused by the re-measurement of the pitch angles by our improved technique, or by revisions of the black hole mass measurements used previously. Both of these changes were quite minor in any case. More importantly, it is not a new trend indicated by the new black hole mass measurements which were unavailable before. Rather, the difference is purely because we are in a position to dispose of the use of masses derived by indirect methods. It should be understood, and it will be shown below, that the results of this paper agree remarkably closely with those previous results when we include those indirect masses used previously. It is only by removing these that we differ at all from the earlier result.

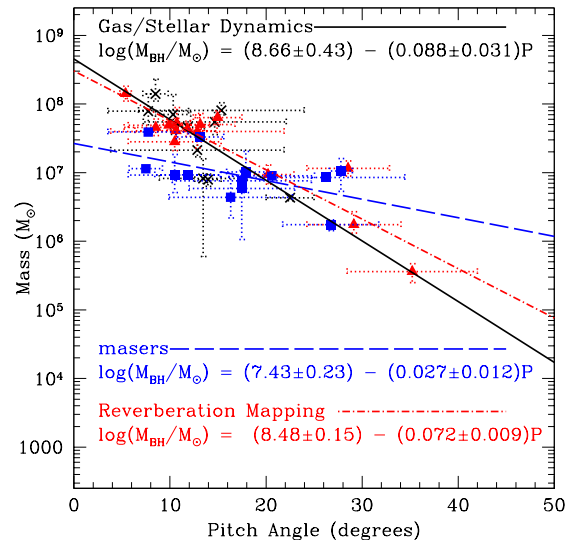


FIG. 2.— Black hole mass vs. pitch angle for all spiral galaxies with directly measured black hole masses available. Black hole masses measured using stellar and gas dynamics techniques (10 points) are labeled with black  $\times$ 's, reverberation mapping masses with red triangles (14 points), and maser measurements with blue squares (13 points). The figure shows three separate fits for the three subsamples. The black solid line is a fit to the gas/stellar dynamics data (black  $\times$ 's), the dashed blue line is a fit to the maser modeling data (blue squares), and the dot-dashed red line is a fit to the reverberation mapping data (red triangles). The gas/stellar dynamics fit and the reverberation mapping fit are fairly compatible and both close to the overall fit. The maser modeling data, however, follows a noticeably shallower slope. Given their small sizes it is difficult to be certain if there is really a conflict between the subsamples.

As we will argue in Section 4, we see the relation between pitch angle and black hole mass as a natural result of density wave theory, which demands that the wavelength of the spiral density waves should depend directly on the mass of the galaxies' central bulge, but this is also true for rival theories. Thus pitch angle, Sérsic index,  $\sigma$ , and bulge luminosity all tend to correlate with each other because they all indirectly measure the central bulge mass. There is strong evidence that this in turn correlates to central black hole mass. It may also ultimately depend on the dark matter halo concentration in some way still to be properly elucidated.

### 3.3. Subsamples of the Full Direct Sample

It is instructive to examine the trends in the overall fits of the three different measurement techniques we have utilized in our data sample. Below, we consider these three techniques separately to verify that each individual subsample provides consistent results. Additionally, this approach allows us to examine any potential differences between active and normal galaxies, as two of our subsample groups consist entirely of active galaxies.

Using only the 10 galaxies with mass estimates utilizing stellar or gas dynamics, which are mostly in normal galaxies, we find a linear fit to the data of the form

$$\log(M_{\text{BH}}/M_{\odot}) = (8.66 \pm 0.43) - (0.088 \pm 0.031)P. \quad (5)$$

This provides a  $\chi^2 = 1.2$  and a scatter of 0.39 dex about the linear fit (Figure 2). This fit differs from the value of Seigar et al. (2008) when only using mass measurements from stellar or gas dynamics, but produces a consistent result, though one with much higher error, and is similarly consistent with our earlier results.

Examining the masers by themselves (Figure 2) results in a

linear fit of the form

$$\log(M_{\text{BH}}/M_{\odot}) = (7.43 \pm 0.23) - (0.027 \pm 0.012)P. \quad (6)$$

The scatter about the fit line for the masers is 0.30 dex. These data is comprised of 13 galaxies with detectable masers, 12 of which have not been measured using stellar and gas dynamics methods.

As we can see from Figure 2, the maser sample has a significantly shallower slope when compared to the direct stellar and gas dynamics measurements. This, combined with the good quality of the fit and low overall scatter, could imply that a separate fit is necessary for this population of active galaxies, but it is difficult to say anything for certain with the relatively small sample size.

Turning to the reverberation mapping subsample, (also in Figure 2) we find a linear fit of the form

$$\log(M_{\text{BH}}/M_{\odot}) = (8.48 \pm 0.15) - (0.072 \pm 0.009)P, \quad (7)$$

with a  $\chi^2 = 0.93$  and a scatter of 0.28 dex for the subsample of 12 reverberation mapped masses alone. This is consistent with the results of Seigar et al. (2008). For an AGN only sample of maser modeling data and reverberation mapping, we find

$$\log(M_{\text{BH}}/M_{\odot}) = (8.09 \pm 0.45) - (0.058 \pm 0.025)P, \quad (8)$$

with a  $\chi^2 = 3.68$  and a scatter of 0.38 dex for this subsample.

The stellar and gas dynamics sample has a somewhat steeper fit than the overall fit, while the maser modeling sample has a somewhat shallower fit. Interestingly, the reverberation mapping sample splits the difference and ends up very close to the overall slope. The steeper fit of the direct, normal subsample may be simply attributable to the fact that this sample lacks smaller black holes and so it is more difficult to determine, on the basis of this sample alone, where the slope really lies.

The reverberation mapping only result shows great similarity to the original fit by Seigar et al. (2008) and is consistent with the fit to stellar and gas dynamics data, with much better scatter. These are significantly different fits from that found using maser data above. They are also consistent with our total sample and the results based on  $M_{\text{BH}} - \sigma$  measurements as we will see in Section 3.4. Meanwhile, the combined maser and reverberation mapping sample produces a result consistent with our other fits, belying any notion that the maser results are different because these objects are AGN.

### 3.4. Comparing $M$ - $P$ Results with $M$ - $\sigma$

Here, we consider one of the most common techniques for estimating galaxy black hole masses, the  $M$ - $\sigma$  relation. This technique is used to estimate the mass of a central SMBH by measuring the velocity dispersion of stars in the galactic bulge. We consider a set of galaxies using the  $M$ - $\sigma$  relation from Ferrarese (2002). This data set utilizes a single fit to the  $M$ - $\sigma$  relation and allows us to fill in portions of the righthand side of the  $M_{\text{BH}}$ -pitch angle relation. We include 23 galaxies from this set, 20 of which do not have direct measurements. These 20 galaxies also includes 3 of the galaxies for which we have mass limits based on stellar or gas dynamics, allowing us to replace those limits (for the purposes of this section) with the mass estimate as derived from the galaxy's  $\sigma$ .

Figure 3 illustrates the results of comparing central velocity dispersion ( $\sigma_c$ ) data with spiral arm pitch angle. The left panel of Figure 3 demonstrates a tight correlation between  $\sigma_c$

and pitch angle. The right panel similarly illustrates a correlation between the 23 masses derived from the  $M$ - $\sigma$  relation of Ferrarese (2002) with pitch angle. The fit to the mass versus pitch angle data is

$$\log(M_{\text{BH}}/M_{\odot}) = (8.47 \pm 0.24) - (0.089 \pm 0.013)P, \quad (9)$$

with a  $\chi^2 = 4.86$  and a scatter of 0.48 dex. This result is consistent with the earlier results based on direct measurements of stellar and gas dynamics as well as reverberation mapping data. Note that while the scatter is high, it is consistent with the scatter found in Gültekin et al. (2009) for the total sample,  $\sim 0.44$  dex, and lower than the result for late-type galaxies alone, 0.56 dex.

Taking the  $\sigma$ -derived masses of the 20 galaxies without direct measurements and adding them to our direct sample of 34 gives us 54 galaxies with mass measurements, either direct or indirect (Figure 4). A fit to these data points gives:

$$\log(M_{\text{BH}}/M_{\odot}) = (8.36 \pm 0.15) - (0.076 \pm 0.008)P \quad (10)$$

with a  $\chi^2 = 10.43$  and a scatter of 0.45 dex (Figure 4.) This result is strikingly close to the result of Seigar et al. (2008)

$$\log(M_{\text{BH}}/M_{\odot}) = (8.44 \pm 0.10) - (0.076 \pm 0.005)P \quad (11)$$

To reiterate, the modest change in the  $M$ - $P$  correlation reported in this paper is entirely due to our decision to drop indirect mass measurements from our sample, because the number of available direct measurements has doubled from the previous work. Thus our results are consistent with the earlier one reported. This, coupled with the fact that the scatter in the relation has improved, suggests that the correlation is not simply the result of an initially small data set.

Therefore, we have two fits to the data to which we attach special importance. The first is our preferred fit that includes all direct measurements and which we adopt as the SMBH  $M$ - $P$  relation. The second includes all direct data plus values of the black hole mass derived from  $\sigma_c$ . It is heartening that the two fits are consistent with each other, though the combined sample has much tighter constraints on the relation even with its modestly larger scatter of 0.45, as opposed to 0.38 dex.

The fit using only direct measurement data has a shallower slope,  $0.062 \pm 0.009$ , than the all-data fit, but the two are fully consistent. Although we place greater faith in the direct data, we must also acknowledge that it is missing a significant amount of data on the right hand side of the relation. Be that as it may, we prefer to rely on the fit based only on direct measurement data for the final result of our correlation.

We now examine how consistent the masses generated from the  $M$ - $P$  relation are with the masses taken from the literature (Figure 5). Those galaxies with upper and lower limits are included in the right panel of the figure. Notice that M33 is a distinct outlier from the rest of the data.

### 3.5. Comparisons with Mass Limits

Finally we look at those galaxies for which only limits are available on their black hole masses. We take a look at the 12 galaxies with upper mass limits set by stellar and gas dynamics effects, as well as 4 galaxies which have lower limits placed on their masses due to estimates of their luminosity in ratio to the Eddington limit, to check for any inconsistencies of the  $M$ - $P$  relation with these mass limits.

As can be seen in the right panel of Figure 5, the limits, with few exceptions, are consistent with the resulting fit. In the cases where the limits are not consistent, we find that they

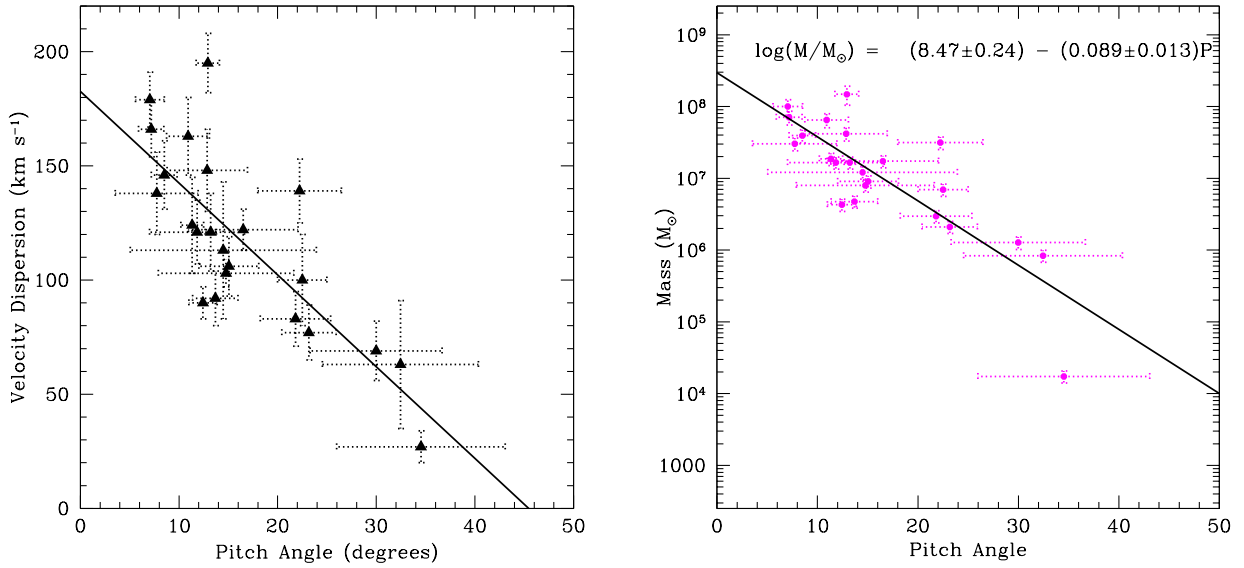


FIG. 3.— Comparisons of pitch angle data with measurements of core stellar velocity dispersion ( $\sigma$ ) for galaxies from Ferrarese (2002). Left:  $\sigma_c$  compared with our measured pitch angles. Right: masses taken from the  $M$ - $\sigma$  relation compared to spiral arm pitch angle. Both figures illustrate a strong correlation between ( $\sigma$ ) and spiral arm pitch angle, as one would expect from our argument that both measure the mass of the galaxy's central bulge (see the Appendix). The fit to the SMBH mass-pitch angle relation is  $\log(M_{\text{BH}}/M_{\odot}) = (8.47 \pm 0.24) - (0.089 \pm 0.013)P$  with a  $\chi^2 = 4.86$  and a scatter of 0.48 dex.

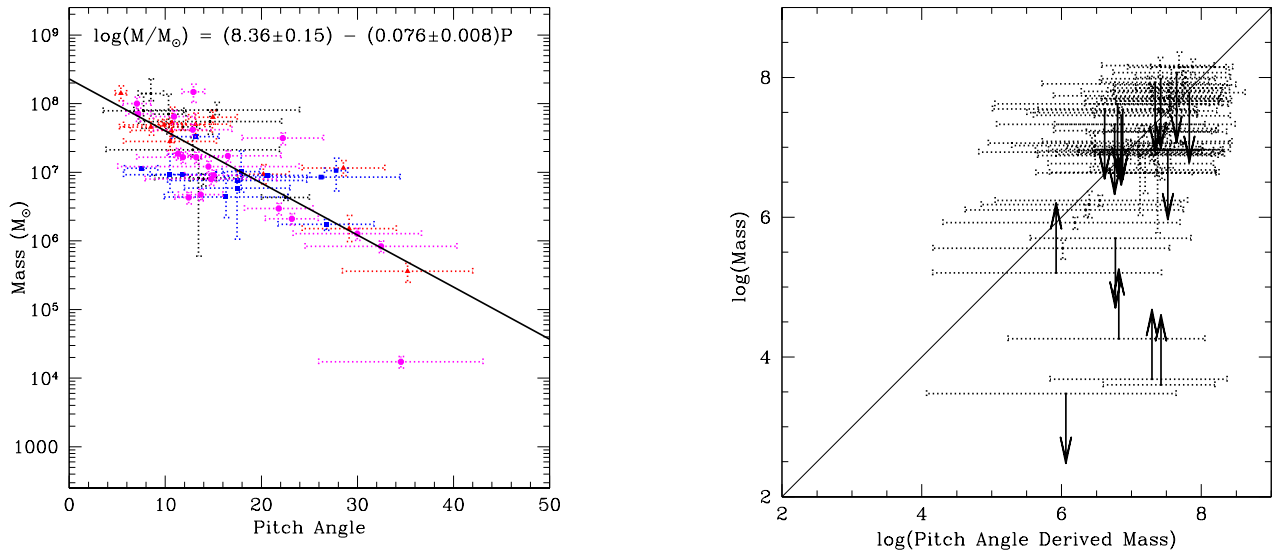


FIG. 4.— SMBH mass-pitch angle relation for all available directly measured black hole masses (as in Figure 1) and for those masses estimated indirectly via  $\sigma$  in our preferred sample (see Table 1 and Section 2.1 for details). The fit to the SMBH mass-pitch angle relation for this extended data set is  $\log(M_{\text{BH}}/M_{\odot}) = (8.36 \pm 0.15) - (0.076 \pm 0.008)P$  with a  $\chi^2 = 10.43$  and a scatter of 0.45 dex. This fit is consistent with that obtained from our sample of directly measured black hole masses (Figure 1) and is almost identical to the fit given in Seigar et al. (2008). The addition of  $\sigma$ -derived masses, several of which are at the low-mass end of our distribution, tends to confirm the validity of the complete sample fit shown in Figure 1 against the much shallower fit found for the maser-modeling-only data shown in Figure 2. Black  $\times$ 's represent data from stellar or gas dynamics (10 points), blue squares represent data from maser modeling (12 points), red triangles come from reverberation mapping data (12 points) and magenta octagons represent masses derived from the  $M$ - $\sigma$  relation (20 points).

are either still consistent with the scatter observed in the fitted points or that the pitch angle is at least more consistent with the measured  $\sigma$  of the galaxy.

M33 has direct estimates which place an upper limit on its mass of  $3.0 \times 10^3 M_{\odot}$  (Merritt et al. 2001). But note that its  $\sigma$  suggests a much greater mass than this, one that is more in line with our correlation (for illustrative purposes this  $\sigma$ -

FIG. 5.— Measured black hole mass of our sample of galaxies compared to the mass derived by applying the fit illustrated in Figure 1 to our measured pitch angles for the same objects. The solid black line is included to illustrate the 1-1 relation, and the distance of each point from the line gives the residual. It will be noticed that some of the limits contradict our fit, as discussed in the text. Two in particular, M33 and IC 342, do so strikingly.

derived value of M33's black hole mass is included in Figure 4 above). Certainly, it would be reasonable to expect, if there is a discrepancy between  $\sigma$  and more direct black hole mass measurements, that the pitch angle would follow  $\sigma$ . Similarly IC 342 has an upper limit mass, based on gas dynamics, of  $M_{\text{BH}} = 5.0 \times 10^5 M_{\odot}$  which contradicts what one would expect from its measured  $\sigma$  (again we included the  $\sigma$ -derived value for IC 342 in Figure 4 above).

The lower limits placed on the sample using the Eddington limit are also illustrated in the right panel of Figure 5. This plot does illustrate that the lower limits placed on the masses by their Eddington luminosities are low, but consistent with the SMBH  $M$ - $P$  relation.

### 3.6. Accuracy of $M$ - $P$ Relation for Estimating Black Hole Masses

In Davis et al. (2012) we show that pitch angle in many cases can be measured to within an accuracy of  $3^\circ$  or lower. This is especially true for grand design spirals, some of which can have pitch angle errors of little over  $1^\circ$ . If we accept  $3^\circ$  as typical of relatively high quality data, then the resulting error in black hole mass estimation obviously depends on the slope of the correlation. A steep slope will translate a modest pitch angle error into quite a large black hole mass error. Fortunately, the correlation is not especially steep. The steepest possible slope consistent with the error in our preferred correlation is  $0.062 + 0.009 = 0.071$ . Thus, an error in pitch angle of  $3^\circ$  translates to a maximum error in the log of the black hole mass of  $0.071 \times 3 = 0.213 M_{\text{BH}}/M_\odot$ . Thus, if we had a pitch angle which translated into a black hole mass of a  $1 \times 10^6 M_\odot$ , such an error would mean that the mass of the black hole, as estimated by our correlation, could vary from  $1.2 \times 10^6 M_\odot$  on the high end to  $7.87 \times 10^5 M_\odot$  on the low end or roughly  $1 \pm 0.2 \times 10^6 M_\odot$  for the case dealt with here; the relative error would be lower for a larger black hole.

In the case of poor quality data or some especially flocculent galaxies, errors can be  $10^\circ$  or higher. In this case the error in black hole mass is  $0.71 M_{\text{BH}}$  and so the same black hole would have a mass, with error of  $(1 \pm 0.71) \times 10^6 M_\odot$ . Therefore pitch angle measurements with errors greater than  $10^\circ$  will do little better than estimating black hole masses to within an order of magnitude.

### 3.7. Sérsic Index

It was shown in Graham et al. (2001) that Sérsic index, which measures the light concentration of a galactic bulge, correlates strongly with black hole mass and in Graham & Driver (2007) a quadratic relation between the log of the Sérsic index and black hole mass was established. Thus, the Sérsic index provides another observational estimate of SMBH masses through images of galactic bulges, and a good competitor to the use of pitch angle measurements in estimating SMBH mass. Certainly, Sérsic index is capable of estimating SMBH masses in early-type galaxies where pitch angle is unusable. The Sérsic indices for several galaxies in our sample, along with corresponding mass estimates from the relation of Graham & Driver (2007) are included in Table 2. We will examine the quality of Sérsic-index-based mass estimates using these values as well as the morphologies of the galaxies.

The left panel of Figure 6 illustrates the relationship between Sérsic index and the pitch angles for galaxies in our sample. In the figure, the black triangles are spiral galaxies without bars, red hexagons are spiral galaxies with weak bars, and blue squares are barred spirals. As can be seen from the figure, there is little apparent correlation between these two properties. This is in contrast to the fairly tight relation between Sérsic-index-produced masses compared to the masses from the literature, see the right panel of Figure 6. Yet, both relations seem to provide reasonable estimates of SMBH mass.

The right panel of Figure 6 compares the masses from the literature with the masses derived from the Sérsic index. The same point types are used in the right panel as the left. A point of interest seems to be the low scatter about the 1:1 line for the regular galaxies when compared to barred galaxies, but that is not surprising since it is more difficult to measure  $n$

in barred galaxies using our isophotal fitting technique. The scatter for the total sample is  $\sim 0.60$  dex, but is strikingly only 0.15 dex for spiral galaxies without bars. This would seem to suggest that Sérsic index is an extremely useful tool in estimating  $M_{\text{BH}}$  for elliptical galaxies and even non-barred early-type spirals. For later-type spirals one has to be extremely careful and adopt the approach of using a multi-component two-dimensional morphological fitting routine (such as GALFIT; Peng et al. 2002). This can become computationally expensive, especially when compared to our approach for determining spiral pitch angles.

The results of this work suggest that for a grand design spiral galaxy the  $M$ - $P$  relation, with its low scatter compared to other methods when applied to spiral galaxies, could be the preferred method of estimating the central black hole mass. This may even prove true for all classes of spiral galaxies. Even if spectroscopic methods are preferred in some cases, a considerable advantage remains that the  $M$ - $P$  relation requires only imaging data, which is becoming plentiful at high quality.

Accurate Sérsic indices still require more image processing and initial estimates to determine, even when a code such as GALFIT (Peng et al. 2002) or BUDDA (de Souza et al. 2004) is used for barred spiral galaxies. In these cases, there are a larger number of parameters that need to be fit, three parameters for the bulge, three for the bar, and two for the disk. A large amount of degeneracy may result, making it more complex to get an accurate handle on the Sérsic index than to measure the pitch angle. These methods have been used to measure large numbers of galaxies (e.g. Gadotti & Kauffmann 2009), but they still require significant time for image processing. As discussed above, unresolved nuclear flux will create difficulties in determining Sérsic index. Automated codes may have difficulties disentangling the unresolved nucleus and the bulge for distant galaxies, which is an issue for several galaxies in our sample. The method of Davis et al. (2012) requires little in the way of image processing in order to measure the pitch angle of the spiral arms, and requires little user input. In the case of late-type non-barred galaxies, Davis et al. (2013) compare SMBH masses (derived from spiral arm pitch angles using the relation here) with Sérsic indices measured from Graham & Driver (2007), and an encouraging result is found. As discussed in Davis et al. (2013), there are strong reasons to prefer the pitch-angle-derived mass function to the Sérsic-index-derived mass function in the case of late-type galaxies. Nevertheless, it is very encouraging that the evidence presented here suggests that Sérsic index and pitch angle estimates of black hole mass are compatible for non-barred spirals. This raises the immediate prospect that a combination of these two approaches (i.e., using Sérsic index for ellipticals and pitch angles for spirals) could produce a black hole mass function for all types of galaxies using imaging data alone. Additionally, a potential method for rapid automated pitch angle measurements in development is discussed in Davis & Hayes (2012).

This comparison provides another opportunity to examine our results. By comparing the residuals, derived by subtracting these results from the masses in the literature, we may elucidate whether the correlations are independent. This will also inform us as to whether the scatter can be reduced through a combination of several parameters. For residuals derived from the linear Sérsic index mass relation of Graham & Driver (2007) versus pitch angle we find a correlation coefficient of  $-0.38$  with 80.4% significance. This is a moderate anti-

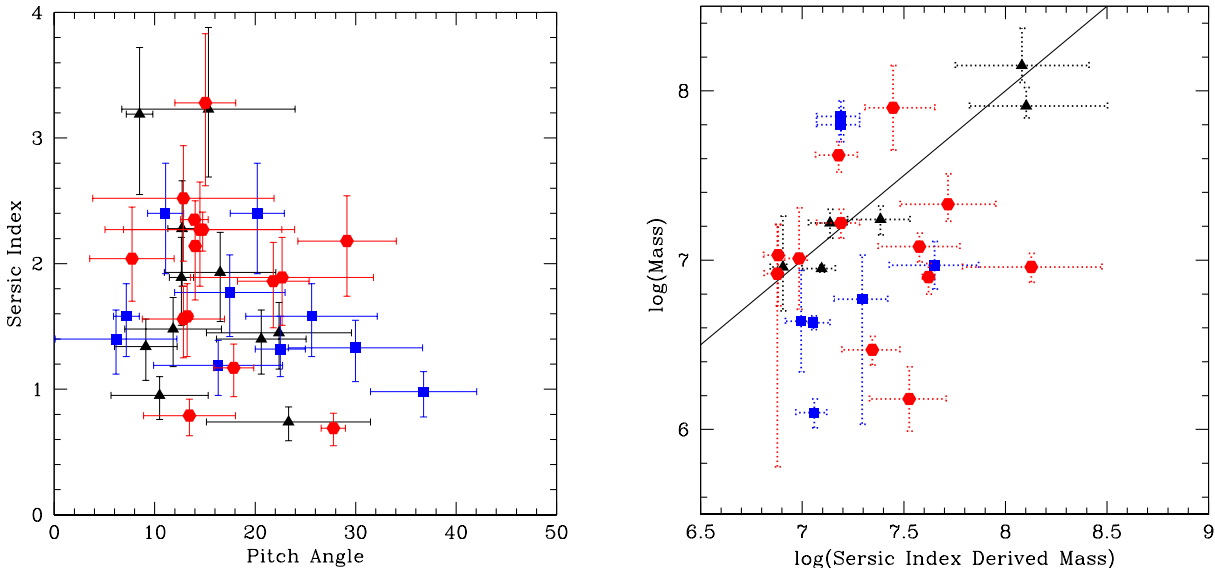


FIG. 6.— *Left*: Sérsic index compared to pitch angle for a subsample of galaxies used in this work. The black triangles represent regular (non-barred) spiral galaxies. Red hexagons are galaxies with morphological classifications as weak bars. Finally, blue squares are barred galaxies. *Right*: a comparison of  $\log(\text{Mass})$  from the literature with the  $\log(\text{Sérsic-index-derived mass})$  using the relationship of Graham & Driver (2007). The solid line through the data represents the 1:1 line. Note that non-barred galaxies have much less scatter about the 1:1 line than either variety of barred galaxy. The scatter for the total sample is  $\sim 0.60$  dex, but is only 0.15 dex for spiral galaxies without bars, 0.73 and 0.72 dex for barred and weakly barred galaxies. No limits are used in this right panel, hence there are fewer points than in the panel on the left.

correlation, but essentially insignificant. Using the preferred quadratic relation from Graham & Driver (2007), the correlation coefficient becomes 0.33 (weak correlation) which is 97.3% significant. This is a greater than  $2\sigma$  result. For pitch angle residuals versus Sérsic index, we find a Pearson rank correlation coefficient of 0.74, with a significance of 99.99%, about a  $4\sigma$  result.

#### 4. DISCUSSION

##### 4.1. Comparisons to Other Methods

In considering the fits to the various categories of data (stellar and gas dynamics, masers, reverberation mapping,  $\sigma$ ), it is notable that the scatter is less than 0.48 dex in all of the samples and subsamples considered. In the case of the direct measurements using stellar or gas dynamics, the scatter is 0.39 dex. This is comparable in scatter to the best of the other galactic features which are known to correlate to black hole mass. In particular, it is comparable to the scatter for the  $M-\sigma$  relation, 0.44 dex, for the full sample of all galaxies in Gültekin et al. (2009). The results of Häring & Rix (2004) produce  $\sim 0.3$  dex scatter using a sample of 30 galaxies. These results rely primarily on early-type galaxies (Ellipticals + S0) to generate these results, as only five of these galaxies are spiral galaxies. This provides us with another useful tool, as bulge luminosity is another imaging-based observable relation that may be complimentary in a full census of SMBH mass. It is true that our correlation holds true only for one category of galaxy (spiral galaxies), but many of the other correlations hold greater uncertainties and scatter for just this type, which is a significant portion of the total population of galaxies. It is further worth noting that the scatter for  $M-\sigma$ , using only late types, is about 0.56 dex, somewhat worse than our scatter (Gültekin et al. 2009). Bulge luminosity and Sérsic index (both of which depend on measurements of the central core of the galaxy) encounter difficulties with spirals, especially barred spirals, where one has to subtract the disk and bar components to find the true bulge component. Routines

such as GALFIT and BUDDA provide powerful tools to make the necessary measurements of the luminosity from bulges (Peng et al. 2002; de Souza et al. 2004). These results may be used with relations such as those from Häring & Rix (2004) and Graham & Driver (2007) to estimate SMBH masses. As one can imagine, the more free parameters you have to fit to the observed surface brightness profiles (and there are at least five in the case of non-barred spiral galaxies, and as many as eight free parameters in barred spirals), the greater the degeneracy between these parameters. As a result, measuring the value of the Sérsic index determined from such fits becomes increasingly complicated. In complex systems (i.e., those with bars and disks, compared to pure bulge or elliptical galaxies), SMBH mass determinations based on pitch angle also appear to be consistent in galaxies with pseudobulges, where other relations appear to break down. It is certainly true that many of the black hole mass functions published to date concentrate first on early types (e.g. Marconi et al. 2004). We intend to use the  $M_{\text{BH}}$ -pitch angle relation to redress this imbalance (Davis et al. 2013). Since spirals will typically have undergone few major mergers in their history in comparison with ellipticals, this technique, which works well for spirals, can help develop information which applies particularly to the accretion history of black holes, as opposed to the merger history.

The fact that various macroscopic and morphological features of galaxies correlate to each other has been noted since galaxies were first observed in any number by Edwin Hubble in the 1920s. Theoretically, the possibility that the black hole at each galaxy's center should correlate with these features is by no means certain but not implausible. A common assertion based upon strong observational evidence is that the mass of the central black hole correlates to the mass of the galaxy's central bulge or core area (e.g., Magorrian et al. 1998; Marconi & Hunt 2003; Häring & Rix 2004; Kormendy et al. 2011). The reason for such a correlation is not settled, though various proposals have been made.

One such proposed mechanism assumes that the depth of the potential in the central region in which the black hole resides governs the amount of available fuel for accretion. If the black hole becomes too large and accretes too rapidly, radiation pressure will force fuel out of the well, thus starving itself of further growth. Thus, the mass of the central region places an upper limit on growth of the black hole (Silk & Rees 1998). As long as the SMBH reaches this limit at some point during its life, its mass should correlate to the mass of its bulge. Recently, it has been suggested that the causal relation is reversed. Instead of the mass of the core controlling the growth of the black hole, it is the mass of the black hole which controls the growth of the core (Jahnke et al. 2009). Either way, the data suggest that such a correlation exists in some form.

Another observable which seems to correlate well with SMBH mass is the Sérsic index of a galaxy ( $n$ ), as discussed above and in Graham et al. (2001); Graham & Driver (2007). The Sérsic index of a galaxy measures the light concentration of a galactic bulge, and thus should correlate to the mass concentration of a galaxy. As we saw in Section 3.7, this relation has potential difficulties when dealing with a large portion of the population of spiral galaxies. This may be a result of the techniques adopted to measure Sérsic index in complicated systems, but this alone may make it difficult to automate the measurement of Sérsic index, whereas techniques to automate the measurement of spiral pitch angle are already being explored (Davis & Hayes 2012). The relation between Sérsic index and SMBH mass is however a complimentary relation that could be used to estimate masses for elliptical and S0 galaxies as well as confirm results on non-barred bulge-dominated spirals.

Since direct measures of black hole masses are intrinsically difficult measurements to make, there is great interest in the use of quantities like bulge luminosity,  $\sigma$ , and  $n$  as markers for the study of a SMBH mass function and its evolution. There is a level of discomfort with the use of such markers that centers around the vast difference between the scale of the black hole (which, in terms of the region of strongly curved spacetime, is similar in size to our solar system, and in terms of the region within which the black hole mass dominates the local stellar mass is only a kiloparsec or so) and the scale of the galaxy's central core (on the order of 10 kpc). Is it really plausible that reliable correlations between quantities on these greatly disparate scales exist? How much more cautious should we be in comparing the same black hole with a quantity whose scale spans the entirety of a disk galaxy, a scale of tens of kiloparsecs?

Nevertheless, there are excellent observational and theoretical grounds for believing that the pitch angle of spiral arms should correlate well with the mass of the galaxy's central bulge despite the significant difference in scale (Lin & Shu 1964; Bertin et al. 1989a,b; Fuchs 1991, 2000; Block et al. 1999; Seigar et al. 2004, 2005, 2006, 2008). Indeed, not only should this relation be causal, but also we can expect it, on theoretical grounds, to be quite tight.

## 5. CONCLUSIONS

We have measured spiral arm pitch angles for a sample of 67 disk galaxies with previously determined SMBH masses. The SMBH masses for these galaxies were taken from a variety of sources which determined the mass via several methods

including (1) direct measurements using stellar or gas dynamics, (2) maser modeling, (3) reverberation mapping, (4) stellar velocity dispersion and the  $M_{\text{BH}}-\sigma$  relation, and (5) Eddington limits for lower mass limits on the SMBHs. The results of several fits to these samples may be found in Table 3. Our main conclusions are as follows.

- Using only galaxies with direct SMBH mass measurements based upon stellar and gas dynamics in normal galaxies as well as maser modeling and reverberation mapping in active galaxies, we find a SMBH mass–pitch angle relation of

$$\log(M_{\text{BH}}/M_{\odot}) = (8.21 \pm 0.16) - (0.062 \pm 0.009)P.$$

- If we include also select indirect black hole mass estimates which were used in the previous correlation studied in Seigar et al. (2008), then we find

$$\log(M_{\text{BH}}/M_{\odot}) = (8.36 \pm 0.15) - (0.076 \pm 0.008)P.$$

This relation is statistically consistent with that presented in Seigar et al. (2008) and virtually identical in slope.

- Our scatter is comparable to, or better than, that in the  $M-\sigma$  relation.
- Our technique does not require observationally expensive spectra. The method is also cosmologically independent, since logarithmic spirals are self similar.
- Using the relationship of Graham & Driver (2007) with a sample of our galaxies illustrates that there is more scatter in Graham's relationship for barred galaxies. Meanwhile, our relationship should not be affected by bars. Thus, two SMBH mass estimators which can take advantage of imaging data only (pitch angle and Sérsic index) are complementary.

Equation 10 is extremely useful for measuring SMBH masses. In Davis et al. (2012), we showed that pitch angle can be measured extremely reliably. In future papers, we intend to use Equation 10 to determine a local SMBH mass function for spiral galaxies (Davis et al. 2013), and for higher- $z$  spirals, provided we can determine how (or if) the SMBH mass–pitch angle relation evolves as a function of look-back time. We can often measure pitch angle to within a relative error of  $3^\circ$  or less. This translates to a relative error in the logarithm of the black hole mass of 4%.

The authors gratefully acknowledge support for this work from NASA Grant NNX08AW03A and NSF REU Site Grant 1157002. This research has made use of the NASA/IPAC Extragalactic Database (NED) which is operated by the Jet Propulsion Laboratory, California Institute of Technology, under contract with the National Aeronautics and Space Administration. The authors also thank Heather Berrier for helpful conversations and suggestions. We are especially grateful to Wayne Hayes and Darren Davis of the University of California at Irvine for measuring a number of our galaxies with their pitch angle code for confirmation purposes and for many helpful discussions on measurement issues.

TABLE 3  
FITTING RESULTS

Sample	Fit	$\chi^2$	Scatter (dex)	Sample Size
Stellar/Gas, Masers, and Reverberation Mapping <sup>a</sup>	$\log(M_{\text{BH}}/M_{\odot}) = (8.21 \pm 0.16) - (0.062 \pm 0.009)P$	4.7	0.38	34
Stellar and Gas Dynamics	$\log(M_{\text{BH}}/M_{\odot}) = (8.66 \pm 0.43) - (0.088 \pm 0.031)P$	1.2	0.39	10
Masers	$\log(M_{\text{BH}}/M_{\odot}) = (7.43 \pm 0.23) - (0.027 \pm 0.012)P$	0.9	0.30	14
Reverberation Mapping	$\log(M_{\text{BH}}/M_{\odot}) = (8.48 \pm 0.15) - (0.072 \pm 0.009)P$	0.9	0.28	14
Masers and Reverberation Mapping	$\log(M_{\text{BH}}/M_{\odot}) = (8.09 \pm 0.45) - (0.058 \pm 0.025)P$	3.7	0.38	28
$M-\sigma$	$\log(M_{\text{BH}}/M_{\odot}) = (8.47 \pm 0.24) - (0.089 \pm 0.013)P$	4.9	0.48	23
All	$\log(M_{\text{BH}}/M_{\odot}) = (8.36 \pm 0.15) - (0.076 \pm 0.008)P$	10.4	0.45	54

NOTE. — Column 1: type of galaxy mass measurements used in the sample. Column 2: sample fit. Column 3:  $\chi^2$  for the fit. Column 4: scatter about the fit in dex. Column 5: number of galaxies in the sample.

<sup>a</sup> This fit represents our preferred fit to the data.

#### APPENDIX

##### SPIRAL DENSITY WAVES AND PITCH ANGLE

In the modal density wave theory it is fairly straightforward to see that the pitch angle of the spiral arms must vary inversely with the mass of the central bulge of the galaxy. From Bertin & Lin (1996) we have

$$\tan i = \frac{m}{rk}, \quad (\text{A1})$$

where  $i$  is the pitch angle of the spiral pattern,  $m$  is the number of spiral arms,  $r$  is the radial position in the disk, and  $k$  is the “local radial wavenumber” which is not constant over the disk but is related to the local wavelength of the density waves by  $\lambda = 2\pi/k$ .

Shu (1984) deals with the case where the pitch angle is relatively small, which is true for Saturn but also for the tightest spiral arms in galaxies, and in the treatment found there one sees how

$$|k| = \frac{D}{2\pi G\sigma_o}, \quad (\text{A2})$$

where  $\sigma_o$  is the surface mass density in the disk and  $D$  is an expression which can be understood as the distance, in frequency terms, from Lindblad resonance of the gravitational potential.

A Lindblad resonance occurs when

$$\omega - m\Omega = \pm\kappa, \quad (\text{A3})$$

where  $\Omega$  is the  $\theta$  (or tangential) frequency of the gravitational potential of the central mass of the galaxy (for a point mass this is  $\Omega = \sqrt{GM}/r^3$ , where  $M$  is the mass of the planet and  $r$  is the radial distance from it) and  $\kappa$  is the epicyclic frequency or radial frequency of the same potential. For a point mass this is the same as  $\Omega$ . Finally,  $\omega$  is a frequency associated with the particle orbiting in this potential, in practice likely to be some kind of forcing frequency which encourages the particle to move with a frequency not quite that of the main potential. For instance, in the case of spiral density waves in Saturn’s rings this  $\omega$  would be associated with the perturbing influence of a nearby moon. Since both  $\Omega$  and  $\kappa$  will vary with radial coordinate  $r$ , it follows that there will only be certain values of  $r$  for which the above relation is satisfied. Such locations are called Lindblad resonances and denoted  $r_L$ . In the theory, spiral density waves emanate from such Lindblad resonances.

The definition of  $D$  is

$$D = \kappa^2 - (\omega - m\Omega)^2 \quad (\text{A4})$$

and clearly at a Lindblad resonance it follows that  $D = 0$ . As a wave moves away from this resonance,  $D$  will no longer be zero. It is easy to show, by a Taylor series expansion, that the key to the pattern of density waves propagating from the resonance is the first derivative of  $D$ .

The details of calculating  $D$  and its derivative are complex because we are dealing with a system which does not encourage the use of the usual simplifying assumptions. The two main frequencies  $\Omega$  and  $\kappa$  are generated by a decidedly non-point source, the central region of the galaxy, and there are many perturbing effects from all of the stars and other material in the disk. Nevertheless, it is obvious that  $D \propto M$  where  $M$  is the mass of the central gravitational source (it would be the mass of Saturn in the case of Saturn’s rings).

Recall that if we have a point mass source, then we would have  $\Omega = \sqrt{GM}/r^3$ . In practice, this is far from the case, but we do expect that  $\Omega = \sqrt{GM}f(r)$  where the particular functional dependence on radial distance is uncertain, but where  $M$  is known to be all of the mass inside the orbit of the particular star or object whose motion we are following. Especially for stars in the inner part of the disk, more specifically for density waves emitted from the inner Lindblad resonance, this  $M$  will be close to the mass of the central bulge of the disk galaxy.

We must also consider the radial frequency of the orbit (which is, in general, eccentric) and we recall that for an orbit in the equatorial plane of an axisymmetric potential

$$\kappa^2 = \frac{1}{r^3} \frac{d}{dr} [(r^2\Omega)^2] = \frac{2\Omega}{r} \frac{d}{dr} (r^2\Omega). \quad (\text{A5})$$

In the point mass case  $\kappa=\Omega$ , but if  $\Omega$  has the generic form given above then we find that

$$\kappa^2 = \frac{2\sqrt{GM}f(r)}{r} \sqrt{GM}(2rf(r) + r^2 df(r)/dr) = 2GM \left( 2f^2 + rf \frac{df}{dr} \right). \quad (\text{A6})$$

Thus provided  $\Omega$  is proportional to  $\sqrt{M}$ , we find that  $\kappa$  will also be proportional to  $\sqrt{M}$ . The frequency  $\omega$  is not so constrained in general, but near the Lindblad resonance it must be close to  $\Omega$  and  $\kappa$  and so it will also be effectively proportional to  $\sqrt{M}$ . Since our density waves originate at the Lindblad resonances, it follows that this is true in our case.

We return to the key quantity  $D$  and begin from

$$D = \kappa^2 - (\omega - m\Omega)^2 = 2GM \left( 2f^2 + rf \frac{df}{dr} \right) - \left( \omega - m\sqrt{GM}f \right)^2. \quad (\text{A7})$$

Since near resonance we expect  $\omega$  to have a value such that the second term on the right is small, we rewrite it as

$$D = 2GM \left( 2f^2 + rf \frac{df}{dr} \right) - GMf^2 \left( \frac{\omega}{\sqrt{GM}f} - m \right)^2. \quad (\text{A8})$$

So we find that  $D \propto M$ , and the derivative of  $D$  with respect to  $r$  will also be proportional to  $M$ , which is (approximately) constant, especially to small changes in radial distance. The fact that  $D \propto M$  means that

$$\tan i \propto \sigma_o/M. \quad (\text{A9})$$

#### REFERENCES

- Athanassoula, E. 2012, MNRAS, L505  
Athanassoula, E., Romero-Gómez, M., Bosma, A., & Masdemont, J. J. 2009a, MNRAS, 400, 1706  
— 2010, MNRAS, 407, 1433  
Athanassoula, E., Romero-Gómez, M., & Masdemont, J. J. 2009b, MNRAS, 394, 67  
Atkinson, J. W., Collett, J. L., Marconi, A., Axon, D. J., Alonso-Herrero, A., Batchelor, D., Binney, J. J., Capetti, A., Carollo, C. M., Dressel, L., Ford, H., Gerssen, J., Hughes, M. A., Macchetto, D., Maciejewski, W., Merrifield, M. R., Scarlata, C., Sparks, W., Stiavelli, M., Tsvetanov, Z., & van der Marel, R. P. 2005, MNRAS, 359, 504  
Barth, A. J. 2004, in Proc. Symp. Coevolution of Black Holes and Galaxies, ed. L. C. Ho (Carnegie Obs. Astrophys. Ser. 1; Cambridge: Cambridge Univ. Press), 21  
Bender, R., Kormendy, J., Bower, G., Green, R., Thomas, J., Danks, A. C., Gull, T., Hutchings, J. B., Joseph, C. L., Kaiser, M. E., Lauer, T. R., Nelson, C. H., Richstone, D., Weistrop, D., & Woodgate, B. 2005, ApJ, 631, 280  
Bentz, M. C., Denney, K. D., Cackett, E. M., Dietrich, M., Fogel, J. K. J., Ghosh, H., Horne, K. D., Kuehn, C., Minezaki, T., Onken, C. A., Peterson, B. M., Pogge, R. W., Pronik, V. I., Richstone, D. O., Sergeev, S. G., Vestergaard, M., Walker, M. G., & Yoshii, Y. 2007, ApJ, 662, 205  
Bentz, M. C., Peterson, B. M., Netzer, H., Pogge, R. W., & Vestergaard, M. 2009a, ApJ, 697, 160  
Bentz, M. C., Peterson, B. M., Pogge, R. W., & Vestergaard, M. 2009b, ApJ, 694, L166  
Bentz, M. C., Walsh, J. L., Barth, A. J., Baliber, N., Bennert, V. N., Canalizo, G., Filippenko, A. V., Ganeshalingam, M., Gates, E. L., Greene, J. E., Hidas, M. G., Hiner, K. D., Lee, N., Li, W., Malkan, M. A., Minezaki, T., Sakata, Y., Serduke, F. J. D., Silverman, J. M., Steele, T. N., Stern, D., Street, R. A., Thornton, C. E., Treu, T., Wang, X., Woo, J.-H., & Yoshii, Y. 2009c, ApJ, 705, 199  
Bertin, G. & Lin, C. C. 1996, Spiral structure in galaxies a density wave theory  
Bertin, G., Lin, C. C., Lowe, S. A., & Thurstans, R. P. 1989a, ApJ, 338, 78  
— 1989b, ApJ, 338, 104  
Blais-Ouellette, S., Amram, P., Carignan, C., & Swaters, R. 2004, A&A, 420, 147  
Block, D. L., Puerari, I., Frogel, J. A., Eskridge, P. B., Stockton, A., & Fuchs, B. 1999, Ap&SS, 269, 5  
Böker, T., van der Marel, R. P., & Vacca, W. D. 1999, AJ, 118, 831  
Booth, C. M. & Schaye, J. 2010, MNRAS, 405, L1  
— 2011, MNRAS, 413, 1158  
Braatz, J. A. & Gugliucci, N. E. 2008, ApJ, 678, 96  
Crenshaw, D. M., Schmitt, H. R., Kraemer, S. B., Mushotzky, R. F., & Dunn, J. P. 2010, ApJ, 708, 419  
Davies, R. I., Thomas, J., Genzel, R., Müller Sánchez, F., Tacconi, L. J., Sternberg, A., Eisenhauer, F., Abuter, R., Saglia, R., & Bender, R. 2006, ApJ, 646, 754  
Davis, B. L., Berrier, J. C., Johns, L., Shields, D. W., Kennefick, D., Kennefick, J. D., Seigar, M. S., & Lacy, C. H. S. 2013, ApJ, Submitted  
Davis, B. L., Berrier, J. C., Shields, D. W., Kennefick, J., Kennefick, D., Seigar, M. S., Lacy, C. H. S., & Puerari, I. 2012, ApJS, 199, 33  
Davis, D. & Hayes, W. 2012, in Computer Vision and Pattern Recognition (CVPR), 2012 IEEE Conference on, 1138–1145  
de Souza, R. E., Gadotti, D. A., & dos Anjos, S. 2004, ApJS, 153, 411  
Denney, K. D., Bentz, M. C., Peterson, B. M., Pogge, R. W., Cackett, E. M., Dietrich, M., Fogel, J. K. J., Ghosh, H., Horne, K. D., Kuehn, C., Minezaki, T., Onken, C. A., Pronik, V. I., Richstone, D. O., Sergeev, S. G., Vestergaard, M., Walker, M. G., & Yoshii, Y. 2006, ApJ, 653, 152  
Denney, K. D., Peterson, B. M., Pogge, R. W., Adair, A., Atlee, D. W., Au-Yong, K., Bentz, M. C., Bird, J. C., Brokofsky, D. J., Chisholm, E., Comins, M. L., Dietrich, M., Doroshenko, V. T., Eastman, J. D., Efimov, Y. S., Ewald, S., Ferbey, S., Gaskell, C. M., Hedrick, C. H., Jackson, K., Klimanov, S. A., Klimek, E. S., Kruse, A. K., Laderoute, A., Lamb, J. B., Leighly, K., Minezaki, T., Nazarov, S. V., Onken, C. A., Petersen, E. A., Peterson, P., Poindexter, S., Sakata, Y., Schlesinger, K. J., Sergeev, S. G., Skolski, N., Stieglitz, L., Tobin, J. J., Unterborn, C., Vestergaard, M., Watkins, A. E., Watson, L. C., & Yoshii, Y. 2010, ApJ, 721, 715  
Devereux, N., Ford, H., Tsvetanov, Z., & Jacoby, G. 2003, AJ, 125, 1226  
Ferrarese, L. 2002, ApJ, 578, 90  
Ferrarese, L. & Merritt, D. 2000, ApJ, 539, L9  
Filippenko, A. V. & Ho, L. C. 2003, ApJ, 588, L13  
Fuchs, B. 1991, in Dynamics of Disc Galaxies, ed. B. Sundelius, 359–363  
Fuchs, B. 2000, in Astronomical Society of the Pacific Conference Series, Vol. 197, Dynamics of Galaxies: from the Early Universe to the Present, ed. F. Combes, G. A. Mamon, & V. Charmandaris, 53  
Gadotti, D. A. & Kauffmann, G. 2009, MNRAS, 399, 621  
Gebhardt, K., Bender, R., Bower, G., Dressler, A., Faber, S. M., Filippenko, A. V., Green, R., Grillmair, C., Ho, L. C., Kormendy, J., Lauer, T. R., Magorrian, J., Pinkney, J., Richstone, D., & Tremaine, S. 2000, ApJ, 539, L13  
Gerola, H. & Seiden, P. E. 1978, ApJ, 223, 129  
Gillessen, S., Eisenhauer, F., Trippe, S., Alexander, T., Genzel, R., Martins, F., & Ott, T. 2009, ApJ, 692, 1075  
Graham, A. W. & Driver, S. P. 2005, PASA, 22, 118  
— 2007, ApJ, 655, 77  
Graham, A. W., Erwin, P., Caon, N., & Trujillo, I. 2001, ApJ, 563, L11  
Grand, R. J. J., Kawata, D., & Cropper, M. 2012, ArXiv e-prints  
Greenhill, L. J., Booth, R. S., Ellingsen, S. P., Herrnstein, J. R., Jauncey, D. L., McCulloch, P. M., Moran, J. M., Norris, R. P., Reynolds, J. E., & Tzioumis, A. K. 2003a, ApJ, 590, 162  
Greenhill, L. J., Kondratko, P. T., Lovell, J. E. J., Kuiper, T. B. H., Moran, J. M., Jauncey, D. L., & Baines, G. P. 2003b, ApJ, 582, L11  
Grosbol, P. J. & Patsis, P. A. 1998, A&A, 336, 840



- Gültekin, K., Richstone, D. O., Gebhardt, K., Lauer, T. R., Tremaine, S., Aller, M. C., Bender, R., Dressler, A., Faber, S. M., Filippenko, A. V., Green, R., Ho, L. C., Kormendy, J., Magorrian, J., Pinkney, J., & Siopis, C. 2009, *ApJ*, 698, 198
- Häring, N. & Rix, H.-W. 2004, *ApJ*, 604, L89
- Harsoula, M. & Kalapotharakos, C. 2009, *MNRAS*, 394, 1605
- Heckman, T. M., Kauffmann, G., Brinchmann, J., Charlot, S., Tremonti, C., & White, S. D. M. 2004, *ApJ*, 613, 109
- Herrnstein, J. R., Moran, J. M., Greenhill, L. J., & Trotter, A. S. 2005, *ApJ*, 629, 719
- Hicks, E. K. S. & Malkan, M. A. 2008, *ApJS*, 174, 31
- Ho, L. C., Li, Z.-Y., Barth, A. J., Seigar, M. S., & Peng, C. Y. 2011, *ApJS*, 197, 21
- Hopkins, P. F., Hernquist, L., Cox, T. J., Robertson, B., & Krause, E. 2007, *ApJ*, 669, 67
- Hu, J. 2008, *MNRAS*, 386, 2242
- Ishihara, Y., Nakai, N., Iyomoto, N., Makishima, K., Diamond, P., & Hall, P. 2001, *PASJ*, 53, 215
- Jahnke, K., Bongiorno, A., Brusa, M., Capak, P., Cappelluti, N., Cisternas, M., Civano, F., Colbert, J., Comastri, A., Elvis, M., Hasinger, G., Ilbert, O., Impey, C., Inskip, K., Koekemoer, A. M., Lilly, S., Maier, C., Merloni, A., Riechers, D., Salvato, M., Schinnerer, E., Scoville, N. Z., Silverman, J., Taniguchi, Y., Trump, J. R., & Yan, L. 2009, *ApJ*, 706, L215
- Jarrett, T. H., Chester, T., Cutri, R., Schneider, S., Skrutskie, M., & Huchra, J. P. 2000, *AJ*, 119, 2498
- Jedrzejewski, R. I. 1987, *MNRAS*, 226, 747
- Kauffmann, G., Heckman, T. M., Budavári, T., Charlot, S., Hoopes, C. G., Martin, D. C., Seibert, M., Barlow, T. A., Bianchi, L., Conrow, T., Donas, J., Forster, K., Friedman, P. G., Lee, Y.-W., Madore, B. F., Milliard, B., Morrissey, P. F., Neff, S. G., Rich, R. M., Schiminovich, D., Small, T., Szalay, A. S., Wyder, T. K., & Yi, S. K. 2007, *ApJS*, 173, 357
- Kaufmann, D. E. & Contopoulos, G. 1996, *A&A*, 309, 381
- Kent, S. M., Dame, T. M., & Fazio, G. 1991, *ApJ*, 378, 131
- Komatsu, E., Smith, K. M., Dunkley, J., Bennett, C. L., Gold, B., Hinshaw, G., Jarosik, N., Larson, D., Nolte, M. R., Page, L., Spergel, D. N., Halpern, M., Hill, R. S., Kogut, A., Limon, M., Meyer, S. S., Odegard, N., Tucker, G. S., Weiland, J. L., Wollack, E., & Wright, E. L. 2011, *ApJS*, 192, 18
- Kondratko, P. T., Greenhill, L. J., & Moran, J. M. 2008, *ApJ*, 678, 87
- Kondratko, P. T., Greenhill, L. J., Moran, J. M., Lovell, J. E. J., Kuiper, T. B. H., Jauncey, D. L., Cameron, L. B., Gómez, J. F., García-Miró, C., Moll, E., de Gregorio-Monsalvo, I., & Jiménez-Bailón, E. 2006, *ApJ*, 638, 100
- Kormendy, J. 1981, in *Cambridge Univ. Press*, Vol. 153, , 111
- Kormendy, J. 1993, in *IAU Symposium*, Vol. 153, *Galactic Bulges*, ed. H. Dejonghe & H. J. Habing, 209
- Kormendy, J. 2004, *Coevolution of Black Holes and Galaxies*, 1
- Kormendy, J. & Bender, R. 2011, *Nature*, 469, 377
- Kormendy, J., Bender, R., & Cornell, M. E. 2011, *Nature*, 469, 374
- Kormendy, J. & Richstone, D. 1995, *ARA&A*, 33, 581
- Kuo, C. Y., Braatz, J. A., Condon, J. J., Impellizzeri, C. M. V., Lo, K. Y., Zaw, I., Schenker, M., Henkel, C., Reid, M. J., & Greene, J. E. 2011, *ApJ*, 727, 20
- Levine, E. S., Blitz, L., & Heiles, C. 2006, *Science*, 312, 1773
- Lin, C. C. & Shu, F. H. 1964, *ApJ*, 140, 646
- Lodato, G. & Bertin, G. 2003, *A&A*, 398, 517
- Macchetto, F., Marconi, A., Axon, D. J., Capetti, A., Sparks, W., & Crane, P. 1997, *ApJ*, 489, 579
- Maciejewski, W. & Binney, J. 2001, *MNRAS*, 323, 831
- Magorrian, J., Tremaine, S., Richstone, D., Bender, R., Bower, G., Dressler, A., Faber, S. M., Gebhardt, K., Green, R., Grillmair, C., Kormendy, J., & Lauer, T. 1998, *AJ*, 115, 2285
- Marconi, A., Axon, D. J., Capetti, A., Maciejewski, W., Atkinson, J., Batcheldor, D., Binney, J., Carollo, C. M., Dressler, L., Ford, H., Gerssen, J., Hughes, M. A., Macchetto, D., Merrifield, M. R., Scarlata, C., Sparks, W., Stiavelli, M., Tsvetanov, Z., & van der Marel, R. P. 2003, *ApJ*, 586, 868
- Marconi, A. & Hunt, L. K. 2003, *ApJ*, 589, L21
- Marconi, A., Risaliti, G., Gilli, R., Hunt, L. K., Maiolino, R., & Salvati, M. 2004, *MNRAS*, 351, 169
- Merritt, D., Ferrarese, L., & Joseph, C. L. 2001, *Science*, 293, 1116
- Miyoshi, M., Moran, J., Herrnstein, J., Greenhill, L., Nakai, N., Diamond, P., & Inoue, M. 1995, *Nature*, 373, 127
- Nowak, N., Thomas, J., Erwin, P., Saglia, R. P., Bender, R., & Davies, R. I. 2010a, *MNRAS*, 403, 646
- . 2010b, *MNRAS*, 403, 646
- Onken, C. A., Valluri, M., Peterson, B. M., Pogge, R. W., Bentz, M. C., Ferrarese, L., Vestergaard, M., Crenshaw, D. M., Sergeev, S. G., Atkinson, J., Batcheldor, D., Carollo, C. M., Collett, J., Dressler, L., Hughes, M. A., Macchetto, D., Maciejewski, W., Sparks, W., & van der Marel, R. 2007, *ApJ*, 670, 105
- Park, D., Kelly, B. C., Woo, J.-H., & Treu, T. 2012, *ArXiv e-prints*
- Pastorini, G., Marconi, A., Capetti, A., Axon, D. J., Alonso-Herrero, A., Atkinson, J., Batcheldor, D., Carollo, C. M., Collett, J., Dressler, L., Hughes, M. A., Macchetto, D., Maciejewski, W., Sparks, W., & van der Marel, R. 2007, *A&A*, 469, 405
- Peng, C. Y., Ho, L. C., Impey, C. D., & Rix, H.-W. 2002, *AJ*, 124, 266
- Peterson, B. M., Bentz, M. C., Desroches, L.-B., Filippenko, A. V., Ho, L. C., Kaspi, S., Laor, A., Maoz, D., Moran, E. C., Pogge, R. W., & Quillen, A. C. 2005, *ApJ*, 632, 799
- Peterson, B. M., Ferrarese, L., Gilbert, K. M., Kaspi, S., Malkan, M. A., Maoz, D., Merritt, D., Netzer, H., Onken, C. A., Pogge, R. W., Vestergaard, M., & Wandel, A. 2004, *ApJ*, 613, 682
- Puerari, I., Block, D. L., Elmegreen, B. G., Frogel, J. A., & Eskridge, P. B. 2000, *A&A*, 359, 932
- Puerari, I. & Dottori, H. A. 1992, *A&AS*, 93, 469
- Roberts, Jr., W. W., Roberts, M. S., & Shu, F. H. 1975, *ApJ*, 196, 381
- Rodríguez-Rico, C. A., Goss, W. M., Zhao, J.-H., Gómez, Y., & Anantharamaiah, K. R. 2006, *ApJ*, 644, 914
- Rosario, D. J., Shields, G. A., Taylor, G. B., Salviander, S., & Smith, K. L. 2010, *ApJ*, 716, 131
- Ryden, B. S. 2004, *ApJ*, 601, 214
- Saraiva Schroeder, M. F., Pastoriza, M. G., Kepler, S. O., & Puerari, I. 1994, *A&AS*, 108, 41
- Sarzi, M., Rix, H.-W., Shields, J. C., McIntosh, D. H., Ho, L. C., Rudnick, G., Filippenko, A. V., Sargent, W. L. W., & Barth, A. J. 2002, *ApJ*, 567, 237
- Satyapal, S., Vega, D., Dudik, R. P., Abel, N. P., & Heckman, T. 2008, *ApJ*, 677, 926
- Satyapal, S., Vega, D., Heckman, T., O'Halloran, B., & Dudik, R. 2007, *ApJ*, 663, L9
- Seiden, P. E. & Gerola, H. 1979, *ApJ*, 233, 56
- . 1982, *Fund. Cosmic Phys.*, 7, 241
- Seigar, M. S., Block, D. L., & Puerari, I. 2004, in *Astrophysics and Space Science Library*, Vol. 319, *Penetrating Bars Through Masks of Cosmic Dust*, ed. D. L. Block, I. Puerari, K. C. Freeman, R. Groess, & E. K. Block, 155
- Seigar, M. S., Block, D. L., Puerari, I., Chorney, N. E., & James, P. A. 2005, *MNRAS*, 359, 1065
- Seigar, M. S., Bullock, J. S., Barth, A. J., & Ho, L. C. 2006, *ApJ*, 645, 1012
- Seigar, M. S. & James, P. A. 1998, *MNRAS*, 299, 685
- Seigar, M. S., Kennefick, D., Kennefick, J., & Lacy, C. H. S. 2008, *ApJ*, 678, L93
- Sérsic, J. L. 1963, *Boletín de la Asociación Argentina de Astronomía La Plata Argentina*, 6, 41
- Shu, F. H. 1984, in *IAU Colloq. 75: Planetary Rings*, ed. R. Greenberg & A. Brahic, 513–561
- Silk, J. & Rees, M. J. 1998, *A&A*, 331, L1
- Springel, V., Di Matteo, T., & Hernquist, L. 2005, *MNRAS*, 361, 776
- Thornley, M. D. 1996, *ApJ*, 469, L45
- Tody, D. 1986, in *Society of Photo-Optical Instrumentation Engineers (SPIE) Conference Series*, Vol. 627, *Society of Photo-Optical Instrumentation Engineers (SPIE) Conference Series*, ed. D. L. Crawford, 733
- Truthardt, P., Seigar, M. S., Sierra, A. D., Al-Baidhany, I., Salo, H., Kennefick, D., Kennefick, J., & Lacy, C. H. S. 2012, *MNRAS*, 423, 3118
- Volonteri, M., Natarajan, P., & Gültekin, K. 2011, *ApJ*, 737, 50
- Wold, M., Lacy, M., Käuffl, H. U., & Siebenmorgen, R. 2006, *A&A*, 460, 449